JOURNAL OF GEOPHYSICAL RESEARCH, VOL. 105, NO. C10, PAGES 24,157-24,181, OCTOBER 15, 2000

# Simulation of water mass formation processes in the Mediterranean Sea: Influence of the time frequency of the atmospheric forcing

S. Castellari[1]
Istituto Nazionale di Geofisica, Roma, Italy

N. Pinardi
Dipartimento di Fisica, Universitá degli Studi di Bologna, Bologna, Italy

K. Leaman
Rosenstiel School of Marine and Atmospheric Sciences, University of Miami, Miami, Florida

**Abstract.** Numerical experiments are conducted to investigate the interannual variability of water mass formation processes in the Mediterranean Sea. The experiments are conducted with a general circulation model which includes a set of calibrated air-sea heat flux bulk formulae to account for the correct surface heat budget of the Mediterranean Basin. An analysis of the model response to different atmospheric forcing frequencies (monthly versus 12-hour) for the period 1980-1988 is conducted in the areas of different water mass formation processes: the Western Mediterranean Deep Water (WMDW), the Eastern Mediterranean Deep Water (EMDW) (only the Adriatic component), the Levantine Intermediate Water (LIW), and the Levantine Deep Water (LDW). All the experiments are able to simulate well the LIW and LDW; however, the 12-hour forced experiments (D experiments) tend to produce more LDW than LIW compared to the monthly forced experiments (M experiments). On the other hand, only the D experiments, with a salinity enhancement, are able in some years to model the WMDW deep convection. The WMDW and EMDW are formed approximately every 3 years depending on the model parameterizations; however, LIW is formed each year but with large-amplitude fluctuations in the volume of water formed. LDW has a formation rate similar to that of deep waters.

## 1. Introduction

The Mediterranean Sea (Med) is one of the few regions in the world ocean where open ocean deep convection occurs. Different kinds of deep water masses are formed through convective processes due to intense winter storms: the Western Mediterranean Deep Water (WMDW) formed in the Gulf of Lions [*MEDOC Group* 1970; *Leaman and Schott*, 1991; *Schott et al.*, 1994, 1996]; the Levantine Deep Water (LDW) formed near the island of Rhodes and detected only recently during the winters of 1987 and 1990 by *Gertman et al.*, [1987, 1994] and during winter 1991 by *Ozsoy et al.*, [1993]; the Eastern Mediterranean Deep Water (EMDW) composed of the Adriatic Deep Water formed in the Southern Adriatic Sea and out-flowing from the Strait of Otranto [*Artegiani et al.*, 1997] and the Aegean Deep Water formed in the Aegean Sea and only detected lately by *Roether et al.*, [1996]. The only intermediate water mass (due to shallow convection up to depths of 200-400 m) is the Levantine Intermediate Water (LIW), formed mainly in the northern Levantine Basin and representing the main thermocline water mass of the Med [*Ovchinnikov*, 1983; *Hecht*, 1986; *Ozsoy et al.*, 1989; Robinson et al., *1991*; *Lascaratos et al.*, 1993].

Generally, surface latent heat fluxes due to winter storms increase the water density in cyclonic gyre locations, thus decreasing the buoyancy and causing the water to sink. In these formation areas the surface air-sea fluxes vary interannually. Here we study the sensitivity of water mass formation to model parameters and to the interannual variability of surface forcing through a set of numerical simulations.

In the last decade, three-dimensional numerical models of the Med water mass formation processes have fo-

[1]Also at ISAO-CNR, Bologna, Italy.



Paper number 2000JC900055.
0148-0227/00/2000JC900055$09.00

cused on the two different subbasins and on the whole basin. An idealized primitive equation model of WMDW formation in the western Mediterranean (WMed) produced a completely vertically homogeneous column of WMDW water in the Balearic-Ligurian Basin using constant climatological thermohaline fluxes [*Madec et al.,* 1991a]. The time scales and space scales of the deep water formation event agreed well with observations, despite the assumptions about forcing (constant and only thermohaline) and convection (parameterized by a nonpenetrative convective adjustment process and Richardson number-dependent vertical eddy viscosity and diffusivity).

Subsequently, the same authors [*Madec et al.*, 1991b] improved their model by introducing variable thermohaline forcing and a finer grid spacing (thus smaller horizontal eddy viscosity and diffusivity coefficients have been possible) and showed that the deep water formation depends on the convective process parameterized and on vertical motion induced by baroclinic instability.

Several model studies have been carried out using the Geophysical Fluid Dynamics Laboratory modular ocean model (GFDL-MOM), referred to as MEDMOM hereafter, [*Pacanowski et al.,* 1991], with a horizontal resolution of 0.25 °, 19 and 31 vertical levels, and open boundary condition at the Strait of Gibraltar.

*Roussenov et al.,* [1995] studied the seasonal variability of the Med circulation by forcing the MEDMOM with climatological momentum and heat fluxes, which were interactively estimated by the model using sea surface temperature (SST). Their model was unable to simulate a correct thermohaline circulation for the Med, both because it lacked deep water formation and because the LIW was too warm. On the other hand, *Zavatarelli and Mellor* [1995] carried out a seasonal simulation of the Med using the Princeton ocean model (POM) forced with prescribed momentum and heat fluxes from *May* [1986] and water fluxes. They were able to simulate LIW and EMDW formation but were unable to reproduce WMDW formation. Later *Pinardi et al.,* [1997] and *Korres et al.,* [2000], using monthly mean atmospheric forcing for 1980-1988 period simulated the horizontal current variability, but they did not describe the water mass production variability. These works are the basis of this study, which now includes the high-frequency, 12-hour atmospheric forcing.

Concentrating more strictly on the water mass formation and spreading processes, *Haines and Wu* [1995] forced the MEDMOM with climatological monthly mean winds and with a relaxation to SST and sea surface salinity (SSS). Their goal was to analyze the climatological water mass formation events and the dispersal of all water masses in the basin. They reproduced LIW with the correct salinity but with warmer temperatures, and a fresher and lighter WMDW, which became an intermediate water. Only the EMDW, flowing out of the Strait of Otranto and spreading south along the Italian coast and east into the southern Ionian Basin, was correctly simulated.

Later, *Wu and Haines* [1996] modified the previous model by introducing a relaxation scheme [*Haney,* 1985] in the Rhodes gyre region to prescribe the LIW formation parameters. They kept standard surface boundary conditions in the rest of the basin, and they used low horizontal viscosity and diffusion coefficients to allow baroclinic eddies to spin up and play an important role in the water mass dispersal. The focus was on the internal dynamics of the Med circulation, and especially on the LIW dispersal and its relation with the deep water mass formation processes. Their simulated LIW was correct and was advected realistically in the rest of the basin, including the southern Adriatic Sea, where by winter the waters were preconditioned for deep convection to occur. In the Balearic-Ligurian Basin the WMDW was formed below 1500 m depth due to the correct lateral advection of LIW.

Finally, *Wu and Haines* [1998], by improving the model setup, were able to carry out a 100-year model integration. In this model the thermohaline circulation reached a state of equilibrium with most of the main water formation processes taking place. The LIW was always above the Sicily sill and reached the WMed, where it contributed to the WMDW formation. This model is the first century timescale non eddy-resolving model to maintain a realistic water mass structure, despite the use of unrealistic surface air-sea interaction physics.

*Nittis and Lascaratos* [1998] focused only on the simulation of water mass processes in the Levantine Basin. Using the POM model, they carried out two experiments, one with climatological and the other with interannual forcing. Both confirmed that the major preconditioning factor for LIW formation is the presence of the Rhodes gyre, and they also showed the LIW formation rate to be about 1.2 Sv. The interannual experiment showed that the LIW formation rate changed according to the intensity of the winter; large decreases were seen during mild winters, while slight increases followed by LDW formation were observed during severe ones. Hence their experiment stressed the importance of short-term extreme atmospheric forcing events compared to the mean climatological events.

The goal of this study is to gain insight into the interannual variability of water mass formation processes of the Mediterranean Sea following the same approach as *Nittis and Lascaratos* [1998], but for the entire Mediterranean. We analyze the response of the MEDMOM to different atmospheric forcing frequencies for the period 1980-1988 (monthly mean and 12-hour). We use the *Pinardi et al.,* [1997] model and study the simulated LIW/LDW, WMDW, and EMDW formation rates caused by different atmospheric forcing frequencies (12-hour versus monthly) for the period 1980-1988.

Section 2 presents an overview of the water mass formation processes. Section 3 describes the model and

**Table 1.** Water Mass Characteristics of Levantine Intermediate Water as Reported by Different Authors

| Authors | T, °C | S, psu | $\sigma_T$ |
|---|---|---|---|
| *Wust* [1961] | 15.50 | 39.10 | 29.05 |
| *Lacombe and Tchernia* [1972] | 15.70 | 39.10 | 28.98 |
| *Ozturgut* [1976] | 16.20 - 16.40 | 39.12 - 39.15 | 28.85 - 28.86 |
| *Ovchinnikov* [1984] | 14.70 - 14.9 | 39.03 - 39.06 | 29.12 - 29.15 |
| *Plakhin and Smirnov* [1984] | 14.50 | 38.85 | 29.06 |
| *Hecht* [1986] | 15.50 ± 0.40 | 39.02 ± 0.05 | 28.91 - 29.01 |
| *Lascaratos et al.,* [1993] | 15.00 - 16.00 | 38.95 - 39.05 | 28.85 - 29.10 |

the atmospheric forcing. Section 4 presents the discussion and the results on the atmospheric fluxes (4.1), the heat budget (4.2), and the different water mass formation processes (sections 4.3 - 4.5). Section 5 presents sensitivity experiments on air-sea interaction physics parameterizations, and section 6 shows the conclusions.

## 2. Water Mass Formation Processes

### 2.1. Levantine Intermediate Water and Levantine Deep Water

During the summer and autumn in the Levantine Basin a warm salty surface layer of Levantine Surface Water (LSW) is present, which increases in density in winter due to cooling. During February and March this mixes with the underlying Atlantic Water (AW) and previously mixed LIW down to depths of 200-400 m, forming the LIW [*Ozsoy et al.*, 1989]. The LIW is the major component of westward flow through the Straits of Sicily and spreads and mixes in the western basin, where it participates in WMDW formation [*Wu and Haines*, 1996]. The location of the LIW formation area has been the subject of several studies [*Lascaratos et al.*, 1993], but the main formation area is thought to be the center of the Rhodes gyre. Lately, *Robinson et al.*, [1991] showed that LIW is present over most of the Levantine Basin but is still preferentially found near the Island of Rhodes. Past studies presented a wide range of values in the definition of the LIW core characteristics, which we review in Table 1.

Recent studies [*Gertman et al.*, 1987, 1994] showed evidence of deep convection occurring in the Rhodes area during the winters of 1987 and 1990, penetrating down to depths of 1000 m in 1987 and 2000 m in 1990. The convection events were produced by strong cooling of the surface waters due to intense winter storms and were characterized by colder temperatures (~ 14°C) and lower salinities (~ 38.85 practical salinity units (psu)) than most of the climatological LIW temperatures and salinities (Table 1). Thus these water masses were classified as LDW, and their characteristics are reported in Table 2.

More recently, *Ozsoy et al.*, [1993] also showed evidence of formation of LDW at the center of the Rhodes gyre during the exceptionally cold winters of 1991 and 1992.

### 2.2. Eastern Mediterranean Deep Water

The Adriatic Sea is considered to be the major source of EMDW. Two different deep water masses are formed there: Dense water is formed during the winter season with T of 12 ± 2°C and S of 38.0 ± 0.5 psu in the northern Adriatic Sea, which then flows to the southern Adriatic Sea, where deep convection and mixing with the incoming LIW takes place. Finally, with a $\sigma_T$ of about 29.20, the newly formed deep water (see Table 3), called Adriatic Deep Water (ADW), exits through the Strait of Otranto, reaches the bottom, and flows along the western boundary of the Ionian Basin becoming EMDW [*Artegiani et al.*, 1989, 1997].

*Ovchinnikov et al.*, [1987] suggested that deep water formation in the Adriatic Sea is intermittent with isolated periods of intense convection and simultaneous overflow through the Strait of Otranto. EMDW is present with near-homogeneous temperature and salinity characteristics everywhere in the eastern Mediterranean (EMed) below an average depth of 1200 m.

A hydrographic survey [*Roether et al.*, 1996] showed that the deep and bottom waters of the EMed changed their characteristics. This was due to a large volume of

**Table 2.** Water Mass Characteristics of Levantine Deep Water as Reported by Different Authors

| Authors | T, °C | S, psu | $\sigma_T$ |
|---|---|---|---|
| *Ozsoy et al.,* [1993] | 13.70 | 38.70 | 29.10 |
| *Gertman et al.,* [1994] | 14.00 - 14.10 | 38.83 - 38.85 | 29.10-29.16 |

**Table 3.** Water Mass Characteristics of Eastern Mediterranean Deep Water as Reported by Different Authors

| Authors | T, °C | S, psu | $\sigma_T$ |
|---|---|---|---|
| *Pollak* [1951] | 13.60 | 38.70 | 29.10 |
| *Ovchinnikov et al.,* [1987] | 13.44-13.75 | 38.70-38.85 | 29.20-29.24 |

deep and bottom water originating in the Aegean Sea, which replaced about 20% of the deep and bottom water previously present in the abyssal Ionian plain. *Roether et al.,* [1996] suggested that changes in the circulation pattern or in the large-scale fresh-water balance in the EMed could have increased the salinity of the Aegean Water, thus affecting the deep water formation of the area. We do not consider this process in our simulations since we integrate only between 1980 and 1988.

### 2.3. Western Mediterranean Deep Water

The WMDW formation has been extensively observed during several "Méditerranée Occidentale (MEDOC)" cruises [*MEDOC Group,* 1970; *Stommel,* 1972] and more recently during a cruise in 1987 [*Leaman and Schott,* 1991; *Schott and Leaman,* 1991] and by "Theoretical and experimental tomography of the sea (THETIS)" Group [*Schott et al.,* 1994, 1996]. A conceptual framework has emerged from the MEDOC studies which have subdivided the WMDW formation process into three phases: a preconditioning phase, a violent mixing phase, and a sinking/spreading phase.

In the preconditioning phase, the presence of a cyclonic gyre in the center of the Gulf of Lions reduces the stability of the surface layer (a distinct doming of isopycnals is present near 42°N and 5°E). This convective patch of water of ~ 100 km diameter defines the specific area of formation (it is approximately at the center of area A in Figure 1).

The violent mixing phase is triggered by the onset of the Mistral (the dry continental northwesterly winds blowing over the area), and the convection takes place in the center of the gyre, producing a neutrally stable water column. The dense surface water mixes with the warmer but saltier subsurface water, leading to a well-mixed water column that sometimes reaches the ocean bottom (~ 2500 m). The area of strong vertical mixing can be identified by values of surface salinity greater than 38.42 psu (Table 4), which indicate the presence of intermediate water mixed up from below [*MEDOC Group,* 1970]. Three or four days after the onset of a strong Mistral the weak stratification at the center of the gyre is eroded, and after about 13 days (at the end of the Mistral) nearly constant values of salinity and temperature with depth are present in the area (see Table 4). *Schott and Leaman* [1991] and *Jones and Marshall* [1993] suggested that during the violent mixing phase the whole water column overturns in numerous plumes (small-scale cells of $\leq$ 1 km horizontal scale), which redistribute cooled surface water in the vertical. These plumes rapidly mix properties over the preconditioned patch, forming a chimney of homogeneous water.

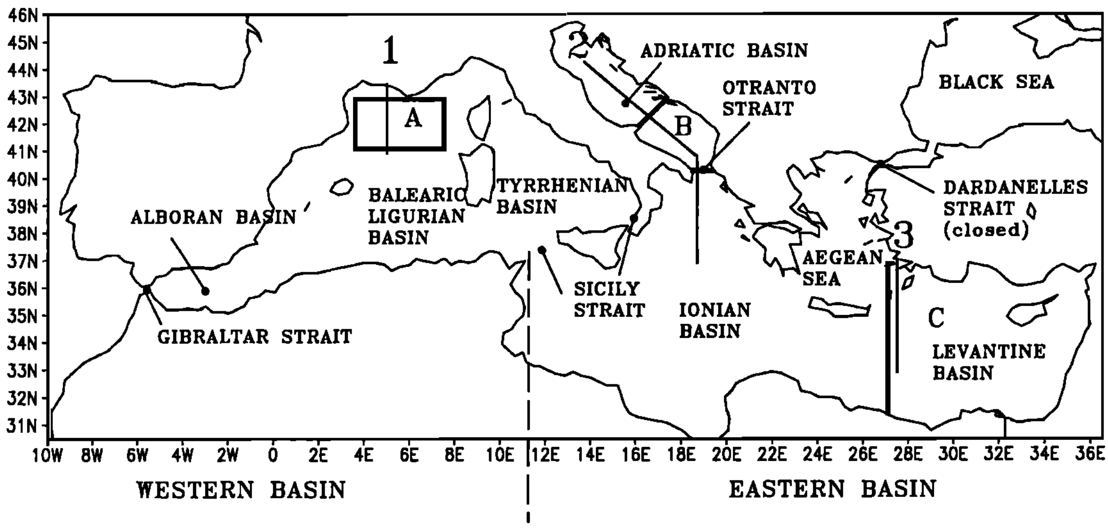


**Figure 1.** Mediterranean Basin nomenclature with the locations of the three sections and the different areas of analysis: Gulf of Lions section (1), south Adriatic-Ionian section (2), Rhodes gyre section (3), WMDW formation area (A), EMDW formation area (B) and Levantine Basin area (C).

**Table 4.** Water Mass Characteristics of Western Mediterranean Deep Water as Reported by Different Authors

| Authors | T, °C | S, psu | $\sigma_T$ |
|---|---|---|---|
| *MEDOC Group* [1970] | 12.70 - 12.90 | 38.42-38.45 | 29.10 |
| *Ovchinnikov et al.,* [1987] | 12.85 | 38.45 | 29.10 |
| *Leaman and Schott* [1991] | 12.80 | 38.44 | 29.10 |
| *Rohling and Bryden* [1992] | 12.70 | 38.40 | 29.10 |

Finally, the sinking/spreading phase is characterized by a breakup of the neutrally stable column of water, followed by a rapid restratification (usually 2 weeks) of the waters at the surface. The newly formed WMDW leaves the formation region, while waters advected by the Ligurian-Provencal Current replace the surface and intermediate waters, and again a three-layer stratification is re-formed [*MEDOC Group,* 1970].

Lately, the effects of convection were studied by *Schott et al.,* [1994, 1996] and *Send et al.,* [1995] with acoustic Doppler current profiler (ADCP) technology. They confirmed the existence of the small-scale plumes during atmospheric cooling, in agreement with the scaling arguments and nonhydrostatic modeling results of *Legg and Marshall* [1993] and *Jones and Marshall* [1993]. In addition, *Schott et al.,* [1994] found that the duration and intensity of the cooling controls the depth range of mixing in the plumes, and that during the sinking/spreading phase the water masses are exchanged with their surroundings through baroclinic instability, creating a large-scale T/S variance lasting up to the next summer. *Send et al.,* [1995] estimated from their observations the volume of convected water and the mean convective depth, and they found that during the winter 1991 the mean formation rate was about 0.3 Sv. Hence the WMDW convection process has three spatial scales: the 50 - 100 km diameter deep mixed patch, the 5 km size of the frontal instability eddies, and the $\leq$ 1 km size of the plumes. In this modeling simulation, only the space scale of the patch can be resolved, since the model horizontal resolution is about 25 km.

Recent studies by *Vaughan and Leaman* [1995] and *Send and Marshall* [1995] pointed out that the plumes themselves only act as mixing agents stirring the water column top to bottom, but with no significant net mean vertical mass transport. *Send and Marshall* [1995] also showed that the convective patch dynamics and water mass formation rates are not dependent on the parameters of the plumes. They suggested, in agreement with previous observations [*Vaughan and Leaman,* 1995], that it is possible to parameterize in hydrostatic models the gross effect of the plumes, as long as these models keep realistic macroscale vertical velocities, instabilities, and water mass distributions and as long as the vertical mixing scheme includes the appropriate mixing plume timescale.

*Mertens and Schott* [1998], by calibrating the available meteorological coastal observations against direct measurements over the Gulf of Lions, derived heat flux time series for the winters from 1969 to 1994. They forced with these heat flux data a one-dimensional mixed layer model initialized by typical preconditioning profiles of early winter and showed significant interannual variability of the convective process driven by the variability of the forcing. Also, they found that the largest negative heat flux of the time series occurred in the winters 1986 and 1987 and that the period 1983-1988 was characterized by large observed mixed layer depths.

## 3. Model Design

The MEDMOM used here has been already applied to realistic simulations of the Mediterranean Sea [*Pinardi et al.,* 1997]. It has a horizontal resolution of 0.25 × 0.25 degrees and 31 vertical levels. The model equations are the Boussinesq, incompressible hydrostatic, and rigid lid Navier-Stokes equations in a rotating frame. The thermodynamics of seawater is represented by the conservation equations for temperature and salinity and the UNESCO equation for density. The equations, formulated in spherical coordinates in the model, are

$$\frac{\partial \mathbf{u}_h}{\partial t} + \mathbf{u} \cdot \nabla \mathbf{u}_h + \mathbf{f} \times \mathbf{u}_h = -\frac{1}{\rho_0}\nabla p - A_M \nabla^4 \mathbf{u}_h + K_M \frac{\partial^2 \mathbf{u}_h}{\partial z^2}, \quad (1)$$

$$\frac{\partial p}{\partial z} = -\rho g, \quad (2)$$

$$\nabla \cdot \mathbf{u} = 0, \quad (3)$$

$$\frac{\partial T}{\partial t} + \mathbf{u} \cdot \nabla T = -A_H \nabla^4 T + K_H \frac{\partial^2 T}{\partial z^2} + \alpha_T(\lambda, \phi, z)(T^* - T), \quad (4)$$

$$\frac{\partial S}{\partial t} + \mathbf{u} \cdot \nabla S = -A_H \nabla^4 S + K_H \frac{\partial^2 S}{\partial z^2} + \alpha_S(\lambda, \phi, z)(S^* - S), \quad (5)$$

$$\rho = \rho(T, S, p), \quad (6)$$

where all the symbols and their definitions are shown in the notation section. The salinity-restoring term $\alpha_S$ is nonzero at the Med surface, in order to relax the salinity field to a monthly climatological observational field ($1 / \alpha_S = 5$ days), and in the selected model region representing the Atlantic box (Figure 1). The relaxation for the sea surface salinity (SSS) has been chosen, instead of the prescribed surface water fluxes dependent on the evaporation-precipitation (E-P) balance, because of the lack of knowledge in precipitation values. Therefore the reference salinity field S* has been taken from the MED2 monthly mean salinity field [*Brasseur et al.*, 1996]. This relaxation implies a water flux $Q_W$ :

$$Q_W = \Delta z_1 (S^* - S)\alpha_S \qquad (7)$$

($\Delta z_1$ is the first model level thickness). The temperature restoring term $\alpha_T$ is different from zero only in the Atlantic box ($1 / \alpha_T = 5$ days). This box parameterizes the inflow of Atlantic Water through the Strait of Gibraltar (Figure 1) and damps the variability in the outflow, allowing the tracer profiles to be relaxed to an annual mean MED2 climatology without imposing any external forcing (a buffer zone boundary condition).

In this study the eddy viscosity and diffusion coefficients have been set, based on sensitivity studies, to $A_M = 8 \times 10^{18}$ cm$^4$/s, $A_H = 2.4 \times 10^{19}$ cm$^4$/s, $K_M = 1.5$ cm$^2$/s and $K_H = 0.3$ cm$^2$/s. The vertical diffusivity coefficient has been chosen small enough to prevent strong mixing in the thermocline layers, while allowing a quite reasonable steep seasonal thermocline. Furthermore, in the case of gravitational instability, $K_H$ goes to infinity and the tracers (T and S in this case) are locally homogenized until neutral stratification is reached, through a numerical scheme termed convective adjustment [*Bryan,* 1969; *Cox,* 1984].

Boundary conditions are supplied for T, S and momentum. At the ocean surface the boundary condition are

$$\rho_0 K_M (\frac{\partial \mathbf{u}_h}{\partial z}) = \mathbf{W}_s, \qquad (8)$$

$$\rho_0 c_p K_H \frac{\partial T}{\partial z} = Q_T, \qquad (9)$$

$$K_H \frac{\partial S}{\partial z} = 0, \qquad (10)$$

$$w = 0, \qquad (11)$$

where $\mathbf{W}_s$ is the wind stress and $Q_T$ is the net surface heat flux or total heat budget. The wind stress is expressed as $\mathbf{W}_s = \rho_A C_D |\mathbf{V}|\mathbf{V}$, where $\rho_A$ is the air density, $C_D$ is the drag coefficient, and $\mathbf{V}$ is the wind velocity. The drag coefficient is calculated as a function of the wind speed and the air-sea temperature difference ($T_A - T_S$) through a polynomial approximation given by *Hellerman and Rosenstein* [1983]. The heat budget $Q_T$ consists of the solar radiation flux ($Q_S$) minus the net long-wave radiation flux ($Q_B$), the latent heat flux ($Q_E$) and the sensible heat flux ($Q_H$). The sea surface temperature (SST) information required for the computation of these fluxes is obtained every time step from the model surface level; this allows an interactive calculation of the surface heat and momentum fluxes of the ocean general circulation model (OGCM). In other words, a feedback exists between the atmosphere and the ocean by forcing with momentum and heat fluxes estimated with the modeled SST. In particular, this model now uses advanced parameterizations of the air-sea interface fluxes developed by *Castellari* [1996]. These advanced parameterizations are described in detail by *Castellari et al.*, [1998] and will not be reproduced here. We say only that the $Q_S$ is parameterized with the *Reed* [1977] formula, $Q_B$ with the *May* [1986] formula, and $Q_E$ and $Q_H$ with the *Kondo* [1975] scheme. They account for the correct long-term mean heat budget of the basin, which was calculated by *Castellari et al.*, [1998] to be equal to - 11 W / m$^2$.

At the bottom of the basin there is an insulating condition for heat and salt, and the friction is set to zero. If bottom flow exists, it is required to be tangent to the bottom slope. The lateral boundary conditions are noslip with insulating walls for heat and salt (no fluxes on the side walls). The initial conditions consist of specifying a density structure through temperature and salinity with the ocean at rest (velocity taken to be zero).

The atmospheric data used to compute the surface heat and momentum fluxes are the 12-hour National Center for Environmental Prediction (NCEP) 1000 mbar analysis (wind velocity $u$ and $v$, air temperature $T_A$, and relative humidity, Rh) and the monthly mean Comprehensive Ocean-Atmosphere Data Set (COADS) cloud cover C, for the period from January 1, 1980, to December 31, 1988. The NCEP data have been averaged monthly over the period of study and then climatologically averaged in order to create a climatological monthly mean data set. The 12-hour NCEP are referred to as the D data and D experiments, and the monthly-averaged NCEP as the M data and M experiments (Table 5).

As mentioned before, the model SSS converges to a prescribed $S^*$ monthly mean distribution; thus the salinity top boundary condition retains the seasonal variability (which includes most of the variance), but does not include shorter-period or interannual oscillations. We have been motivated to introduce a salinity correction which increases the SSS values in the A area (Figure 1) during deep water preconditioning (usually in January in our experiments) and violent mixing (usually in February and March) phases. This salinity correction has been applied in both the M and D experiments and these last two experiments are referred to as the MS and DS experiments in Table 5. This correction is needed since no proper LIW dispersal is occurring in our model, but WMDW formation is strongly related to LIW, arriving in the Gulf of Lions [*Wu and Haines,*

**Table 5.** The Different Numerical Experiments Showing the Atmospheric Forcing Data, the Heat Flux formulae, and the Salinity Flux Used

| Experiment | Atmospheric Forcing | Heat Flux Formulae | Salinity Flux |
|---|---|---|---|
| M | 1980-1988 monthly mean NCEP | standard | $S^*$ |
| MS | 1980-1988 monthly mean NCEP | standard | modified $S^*$ |
| D | 1980-1988 12-hour NCEP | standard | $S^*$ |
| DS | 1980-1988 12-hour NCEP | standard | modified $S^*$ |
| DS1 | 1980-1988 12-hour NCEP | modified 1 | modified $S^*$ |
| DS2 | 1980-1988 12-hour NCEP | modified 2 | modified $S^*$ |

"Standard" corresponds to $Q_S$ by Reed;[e] $Q_B$ by May;[d] $Q_E$ and $Q_H$ by Kondo.[c] "Modified 1" corresponds to standard except for $Q_B$ by Brunt-Berliand,[b] and "modified 2" corresponds to standard except for $Q_B$ by Berliand-Berliand.[a]

[a] *Berliand and Berliand* [1952].
[b] *Budyko* [1974].
[c] *Kondo* [1975].
[d] *May* [1986].
[e] *Reed* [1977].

1996]. Thus we increase the SSS to mimic the presence of LIW in the subsurface. The details of the convection process itself will not be properly modeled by our parameterization, but hopefully the net result, after deep convective mixing, will be the same.

The MED2 SSS values interpolated on the MOM grid have been taken for the A area for the months of January and February and the surface averages and the corresponding standard deviations have been computed in the area. The standard deviations $\mathrm{STD}_S^{jan}$ and $\mathrm{STD}_S^{feb}$ are 0.14 psu and 0.16 psu respectively. These values have been added to the climatological MED2 salinity field in the A area, modifying the last term on the right-hand side of equation (5) to $\alpha_S(S^\star + STD_S - S)$. This has been done only in A area grid points and for the months of January and February of each year. Furthermore, in the A area and only during January and February the relaxation coefficient has been changed to $\alpha_S = d^{-1}$ with d = 2 hours.

The M, MS, D, and DS experiments have all used our standard air-sea interaction formulae as described before. Two more experiments have been done with different air-sea interaction physics to show the sensitivity of model results to these important parameterizations. These experiments are called DS1 and DS2 in Table 5, and they will be described later.

## 4. Results

### 4.1. Interannual Variability of Atmospheric Fluxes

In order to analyze the interannual variability of the model forcing, we have estimated the surface integrals of wind stress, wind stress curl, and heat budget over the Mediterranean Basin (Figure 2) extracted from the M and D experiments. These atmospheric fluxes, as already mentioned, are estimated from the model by using the model SST in the calculation of the different fluxes.

Figure 2a shows a strong interannual variability in the wind stress forcing, with the largest peak in the winter of 1981 and others in 1986 and 1987. The summer Etesian winds can be detected in the wind stress time series from the secondary peaks located in the summer months, with the largest peaks in 1981, 1982, and 1984.

By analyzing the wind stress curl time series (Figure 2b), it is possible to notice that the largest vorticity inputs occur in the winters of 1981 and 1986, and that the curl is amplified in the D experiment.

Figure 2c shows the surface integrals of $Q_T$ anomalies with respect to the seasonal cycle over the Med for different experiments. Negative anomalies are evident during the winters of 1981 (January), 1987 (March), and 1988 (March), and positive anomalies are evident in the summers 1987 and 1988 in both the M and D experiments.

By analyzing the two Mediterranean subbasins separately for the D experiment (Figure 3), we note that the wind stress peak in the winter of 1981 is largest in the EMed, while the peak in the winter of 1986 is strongest in the WMed (Figure 3a). Figure 3b shows the same difference in the wind stress curl.

The negative heat budget anomaly of winter 1981 is of almost equal magnitude in both subbasins, while the winter 1987 heat budget anomaly is larger in the WMed than in the EMed (Figure 3c).

In summary, the surface heat and momentum fluxes show two large anomalies centered during the winter season (1981 and 1987) and two large summer anomalies (1987 and 1988).

### 4.2. Heat Budget

We have decided to analyze the simulated surface heat budget of the main numerical experiments, as

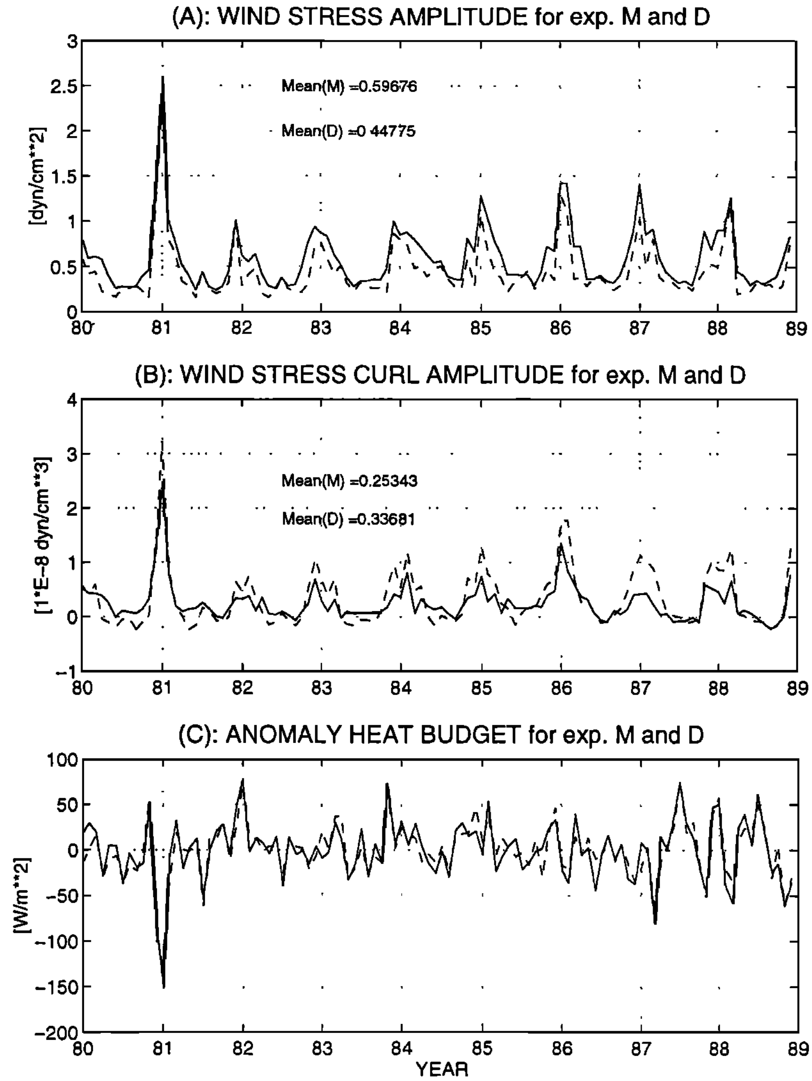


**Figure 2.** Experiment M (solid line) and experiment D (dashed line): surface integrals over the Mediterranean Sea of (a) wind stress amplitude (dyn/cm$^2$), (b) wind stress curl amplitude ($1 \times 10^{-8}$ dyn/cm$^3$), and (c) surface heat budget anomalies (W/m $^2$).

a parameter to control the overall consistency of the model experiments. The annual and climatological (9-year mean) surface integrals of $Q_T$ for the main four experiments are studied, and the climatological means are compared to the climatological $Q_T$ estimates from previous studies (Table 6). Only *Bethoux* [1979] and *Bunker et al.*, [1982] estimated with observational data heat losses for the Med, that were consistent with the net heat flux through the Strait of Gibraltar. Other authors reached positive heat budgets [*May*, 1986; *Garrett et al.*, 1993; *Gilman and Garrett*, 1994]. On the other hand, *Castellari et al.*, [1998], by using the same data sets of this study along with *Reynolds* [1988] SST monthly means, obtained a negative heat budget of -11 W/m $^2$.

Table 7 and Table 8 show the surface heat budgets (annual, winter, and summer means) of the main experiments. The climatological annual heat budgets are all negative, with values around -5 W/m $^2$ for the M and MS experiments, and around -10 W/m $^2$ for the D and DS experiments. The climatological annual heat budgets of the D and DS experiments are consistent with the *Castellari et al.*, [1998] results obtained with the same atmospheric data, observed SST and bulk formulae. By analyzing the heat budgets of Tables 7, and 8 we can define for all experiments two cold periods (with large heat losses at the sea surface) in 1980-1981 and 1986-1988, and one warm period, 1982-1985 (with small heat loss or heat gain at the sea surface). All experiments show that the coldest winters are in years 1981 and 1987, while the warmest summers are in years 1987 and 1988. These model climatological annual heat budgets show large standard deviations of about 6.8-8. W/m $^2$, indicating the strong interannual variability of the simulated heat budgets. In general, the high-frequency forcing (D and DS experiments) compared to the low-frequency forcing (M and MS experiments) produces lower heat budget values, thereby keeping the

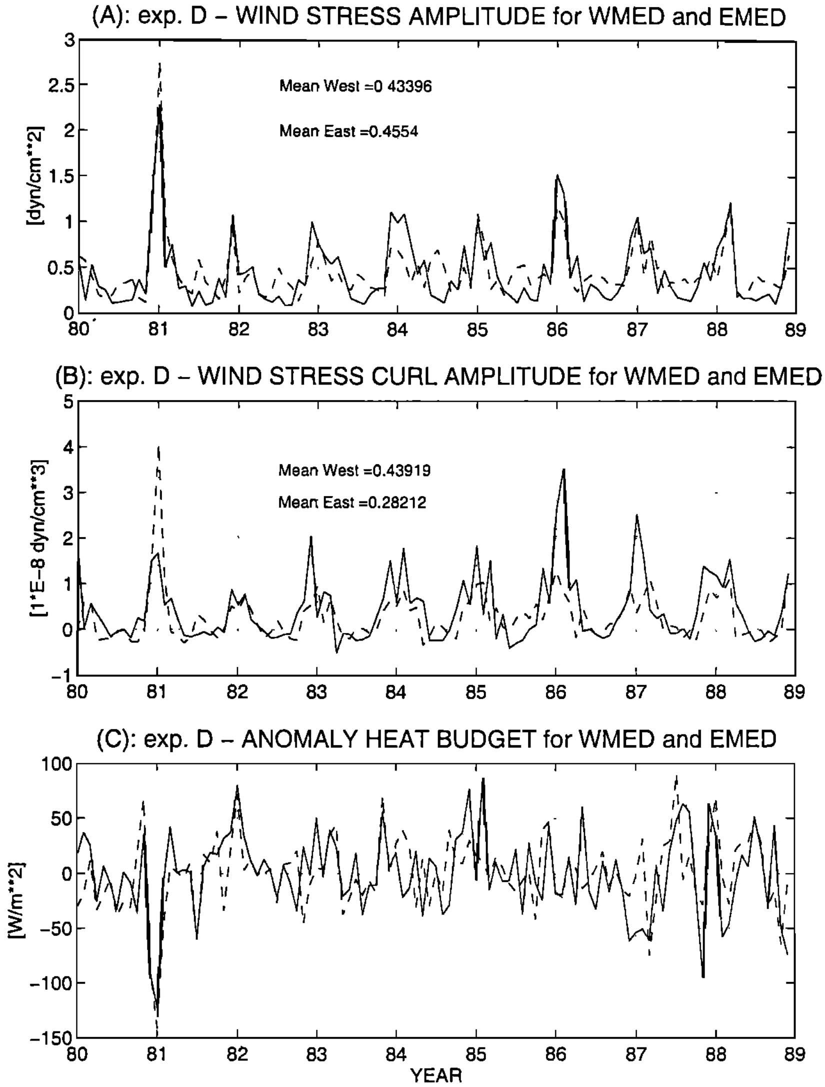


**Figure 3.** Experiment D: surface integrals over the western Mediterranean (WMed) (solid line) and eastern Mediterranean (EMed) (dashed line) of (a) wind stress amplitude (dyn/cm$^2$), (b) wind stress curl amplitude ($1 \times 10^{-8}$ dyn/cm$^3$), (c) and surface heat budget anomalies (W/m $^2$).

interannual fluctuations of the same order (the standard deviation is almost the same).

We have also estimated the surface integrals of the water fluxes $Q_W$ for the four experiments; all are about 0.40 m/yr for the period 1980-1988, which are 30% lower than observational values 0.63 - 0.69 m/yr for the period 1968-1973 as calculated by *Peixoto et al.,* [1982].

**Table 6.** Mediterranean Long-Term Mean Heat Budget

| Authors | $Q_T$ |
|---|---|
| *Bethoux* [1979] | -6 |
| *Bunker et al.,* [1982] | -7 |
| *May* [1986] | 2 |
| *Garrett et al.,* [1993] | 29 |
| *Gilman and Garrett* [1994] | 0 |
| *Castellari et al.,* [1998] | -11 |

## 4.3. Levantine Intermediate Water and Levantine Deep Water Formation

We analyze a north-south section through the Rhodes gyre (3 of Figure 1), by computing the largest depth of outcropped LIW density layers between 28.85 and 29.10, which represents the climatological LIW density (Table 1). In Table 9 we show the depths of this layer in February of each year. The M experiment typically simulates shallow convection, down to 400 m (typical of LIW), while the D experiment shows deeper convection to 800 m.

In the M experiment the shallow LIW convection is centered around 33°N and reaches depths of about 400 - 700 m with water characteristics of T ~ 14.75° - 14.80°

**Table 7.** Mediterranean Heat Budget $Q_T$ for experiments M, and MS

| | M | | | MS | | |
|---|---|---|---|---|---|---|
| Year | Annual | Winter | Summer | Annual | Winter | Summer |
| 1980 | −10.4 | −62.9 | 58.5 | −14.7 | −62.2 | 58.5 |
| 1981 | −12.5 | −126.2 | 67.5 | −15.0 | −126.4 | 67.3 |
| 1982 | 0.7 | −54.9 | 68.5 | −2.3 | −55.1 | 68.4 |
| 1983 | −1.0 | −78.7 | 78.5 | −3.3 | −79.3 | 78.5 |
| 1984 | 2.3 | −63.1 | 75.2 | 1.9 | −63.9 | 75.0 |
| 1985 | −0.3 | −76.6 | 66.2 | −0.1 | −77.1 | 66.1 |
| 1986 | −15.6 | −91.1 | 78.8 | −15.5 | −91.9 | 78.4 |
| 1987 | 1.3 | −109.4 | 117.5 | −2.8 | −110.1 | 117.2 |
| 1988 | −7.6 | −100.3 | 97.3 | −7.3 | −100.4 | 97.3 |
| Mean | −4.8 | −84.8 | 78.7 | −5.1 | −85.2 | 78.5 |
| s.d. | 6.8 | 23.8 | 18.3 | 6.8 | 23.9 | 18.2 |

Climatological mean and standard deviation (s.d.) for each year, each winter, and each summer are given for different numerical experiments. Values are in Watts per square meter.

C and S ~ 38.85 - 38.90 psu (Figure 4), which produce densities of ~ 29.04 - 29.06 (Figures 6a, 6c, and 6e). The D experiment shows a tendency to produce a large quantity of LIW with lower temperatures (T ~ 14.20° - 14.60°C) as well as LDW. The latter is produced with water characteristics of T ~ 13.75° - 14.25°C and S ~ 38.85 - 38.90 psu (Figure 5), which produces densities close to 29.10 (Figure 6 b, 6d, and 6f), similar to Table 2 values.

Hence the D experiment shows that with strong sea surface cooling due to high-frequency atmospheric forcing, large amounts of LDW can be formed in a deep convection scenario similar to that of the WMDW in the WMed. The larger densities in the D experiment are produced by colder temperatures rather than higher salinities. In all experiments the salinity values are in fact slightly lower than the climatological LIW salinity range (38.92-39.15 psu).

It is of interest to estimate the LDW and LIW formation rate variability due to the atmospheric forcing. In order to do so, the maximum volume of newly formed water with $\sigma_T$ ranging between 28.95 and 29.10 present in the mixed layer over the Levantine Basin (area C in Figure 1) has been computed, and then divided by 1 year. The same has been done for the formation rate of LDW with $\sigma_T$ larger than 29.10. This gives a yearly formation rate in sverdrups (Sv) under the assumption of nonpenetrative convection. *Lascaratos et al.*, [1993] using the same procedure, estimated the LIW formation rate to be 1.0 Sv from a climatologically forced mixed layer model. In another way, *Tziperman and Speer* [1994] estimated the LIW formation rate to be about 1.5 Sv. Figure 7 shows the strong interannual variability of the LIW formation rate for our experiments. LIW is formed each year at a relevant rate, with the smallest formation rate in 1984, and the largest in

**Table 8.** Mediterranean Heat Budget $Q_T$ for experiments D, and DS

| | D | | | DS | | |
|---|---|---|---|---|---|---|
| Year | Annual | Winter | Summer | Annual | Winter | Summer |
| 1980 | −22.8 | −101.0 | 49.8 | −22.9 | −101.1 | 49.8 |
| 1981 | −20.6 | −151.4 | 63.8 | −20.9 | −151.9 | 63.7 |
| 1982 | −4.1 | −68.3 | 70.9 | −4.0 | −68.3 | 71.1 |
| 1983 | −4.0 | −82.2 | 65.5 | −3.7 | −81.0 | 65.5 |
| 1984 | −1.1 | −83.5 | 74.1 | −0.9 | −82.3 | 74.1 |
| 1985 | −3.6 | −88.3 | 72.7 | −7.8 | −89.3 | 71.3 |
| 1986 | −15.9 | −109.7 | 74.2 | −15.4 | −118.1 | 77.0 |
| 1987 | −7.4 | −130.7 | 117.0 | −7.7 | −132.1 | 117.3 |
| 1988 | −8.4 | −101.4 | 90.0 | −9.4 | −101.2 | 91.2 |
| Mean | −9.8 | −101.8 | 75.3 | −10.3 | −102.8 | 75.7 |
| s.d. | 8.0 | 25.9 | 18.9 | 7.8 | 26.9 | 19.2 |

Climatological mean and standard deviation (s.d.) for each year, each winter, and each summer are given for different numerical experiments. Values are in Watts per square meter.

**Table 9.** Depth of Levantine Intermediate Water

| Year | M | D |
|---|---|---|
| 1980 | ~ 400 m | ~ 400 m |
| 1981 | ~ 700 m | ~ 900 m |
| 1982 | ~ 700 m | ~ 800 m |
| 1983 | ~ 600 m | ~ 800 m |
| 1984 | ~ 500 m | ~ 600 m |
| 1985 | ~ 400 m | ~ 600 m |
| 1986 | ~ 600 m | ~ 600 m |
| 1987 | ~ 600 m | ~ 800 m |
| 1988 | ~ 500 m | ~ 500 m |

Criterion is outcropping of layers with $\sigma_T$ between 28.85 and 29.10 for February of each year. The depth indicates where the deepest isopycnal of 28.85 – 29.10 is located before it outcrops.

1987 for the M experiment and in 1981 for the D experiment.

In general, both experiments show a tendency to produce large volumes of LIW in the Levantine Basin at an average climatological rate of several times the climatological values. In section 5 we show that the average rate can be reduced toward the estimated values of 1-1.5 Sv by using different air-sea interaction physics parameterization on the model surface, but the annual frequency remains the same. However, we have to remember that our estimate of interannual production may be also affected by the coarse resolution used, as found by *Nittis and Lascaratos* [1998].

A tendency to produce LDW as the model integrates forward is present in the D experiment. However, the frequency of LDW production is smaller than LIW, with only two large peaks in 1983 and 1987. Even if there is a large drift in the LDW production rate, we may

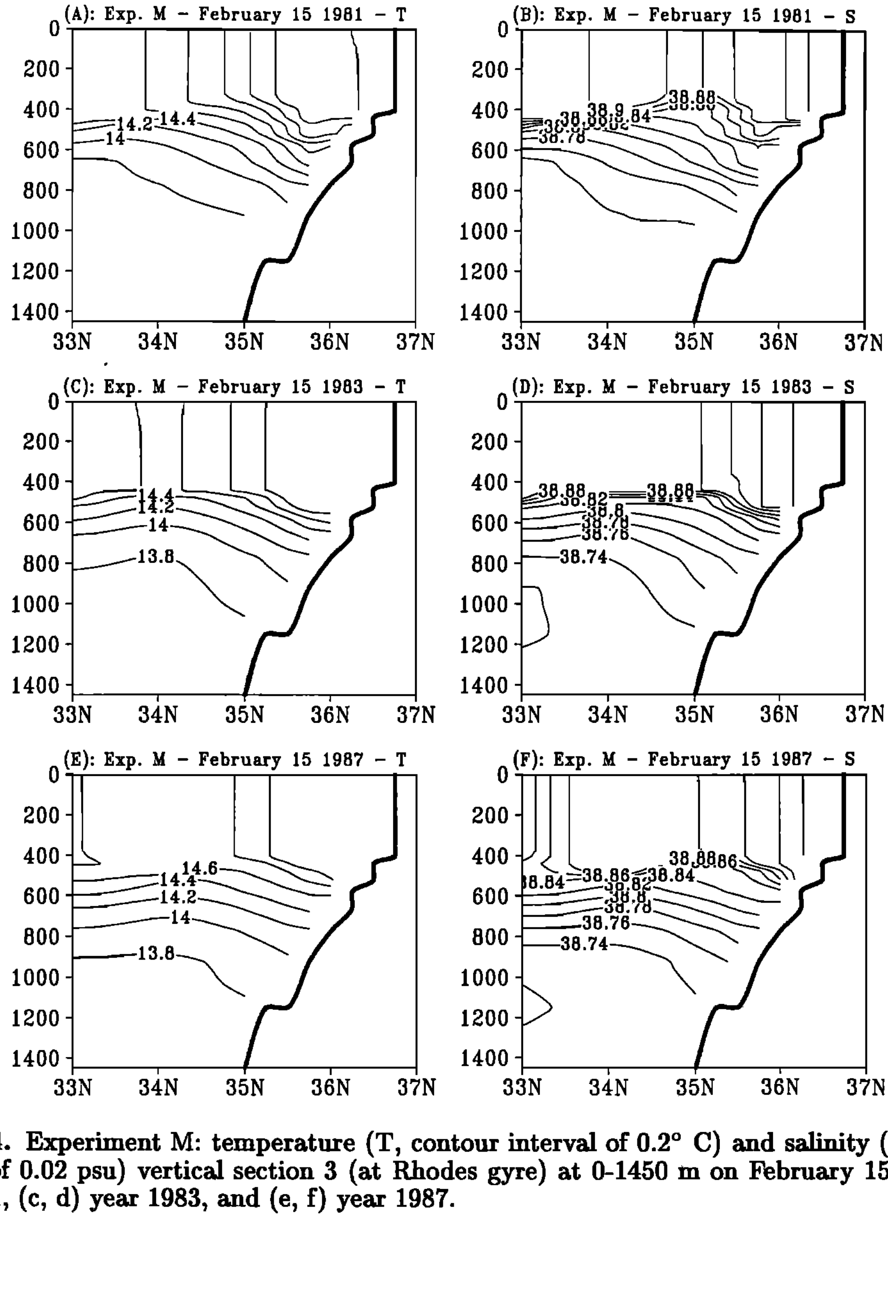


**Figure 4.** Experiment M: temperature (T, contour interval of 0.2° C) and salinity (S, contour interval of 0.02 psu) vertical section 3 (at Rhodes gyre) at 0-1450 m on February 15 for (a, b) year 1981, (c, d) year 1983, and (e, f) year 1987.

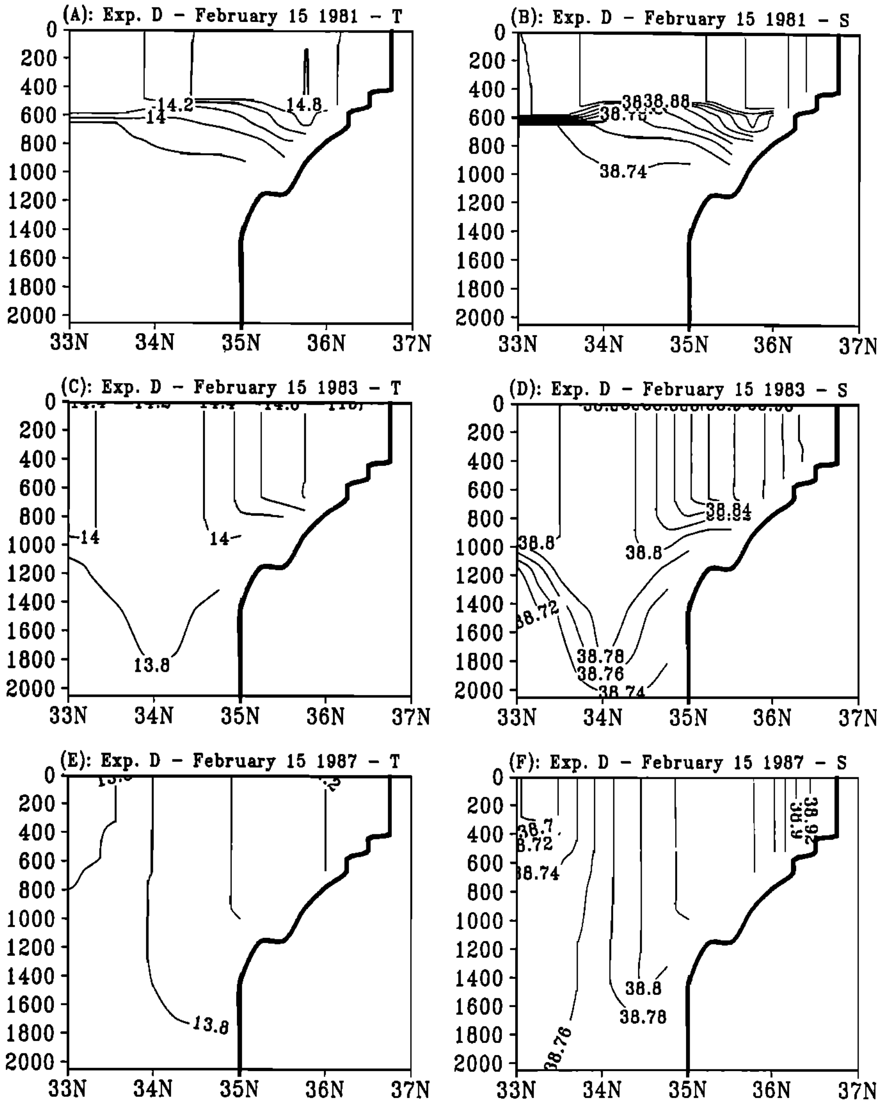


**Figure 5.** Experiment D: temperature (T, contour interval of 0.2° C) and salinity (S, contour interval of 0.02 psu) vertical section 3 (at Rhodes gyre) at 0-2050 m on February 15 for (a, b) year 1981, (c, d) year 1983, and (e, f) year 1987.

argue that LDW production is more sporadic in time than LIW production. During the years 1987, 1990, 1991, and 1992, some studies [*Gertman et al.*, 1987, 1994; *Ozsoy et al.*, 1993] have shown evidence of LDW production along with LIW production in the Rhodes area. No previous evidence of LDW events is available in the literature. We think, despite possible problems in the model, that the frequency of LDW production in the years 1983 and 1987 present in the D experiment is consistent with the past observations.

### 4.4. Eastern Mediterranean Deep Water Formation

We analyze the EMDW formation in the Adriatic through the vertical section 2 (Figure 1). Table 10 shows the depth of the EMDW outcropped density layers (in the range 29.10 - 29.20) in the southern Adriatic area. The M experiment produces deep convective events only in the winters of 1981, 1987, and 1988, while in the other years the mixing reaches only 600 m depth (Table 10). We show (Figures 8-10) vertical sections for the years 1981, 1987 (as examples of strong convective events), and 1985 (as an example of weak convective events). The density isopycnals larger than 29.00 but less than 29.15 outcrop in all years except for 1987, when even the isopycnals larger than 29.20 outcrop (Figure 8 a, 8c, and 8e). The newly formed water which flows out of the Strait of Otranto reaches a depth of 800-1000 m in the Ionian Basin in 1981 and 1987, while in other years it reaches shallower depths around 600 m. Generally, compared to the values of Table 3, temperature values of the southern Adriatic newly formed water are lower than observations by about a degree (Figure 9 a, 9c, and 9e), and salinity values are lower by 0.3 - 0.4 psu (Figures 9b, 9d, and 9f). Hence the density of the newly formed EMDW is lower than

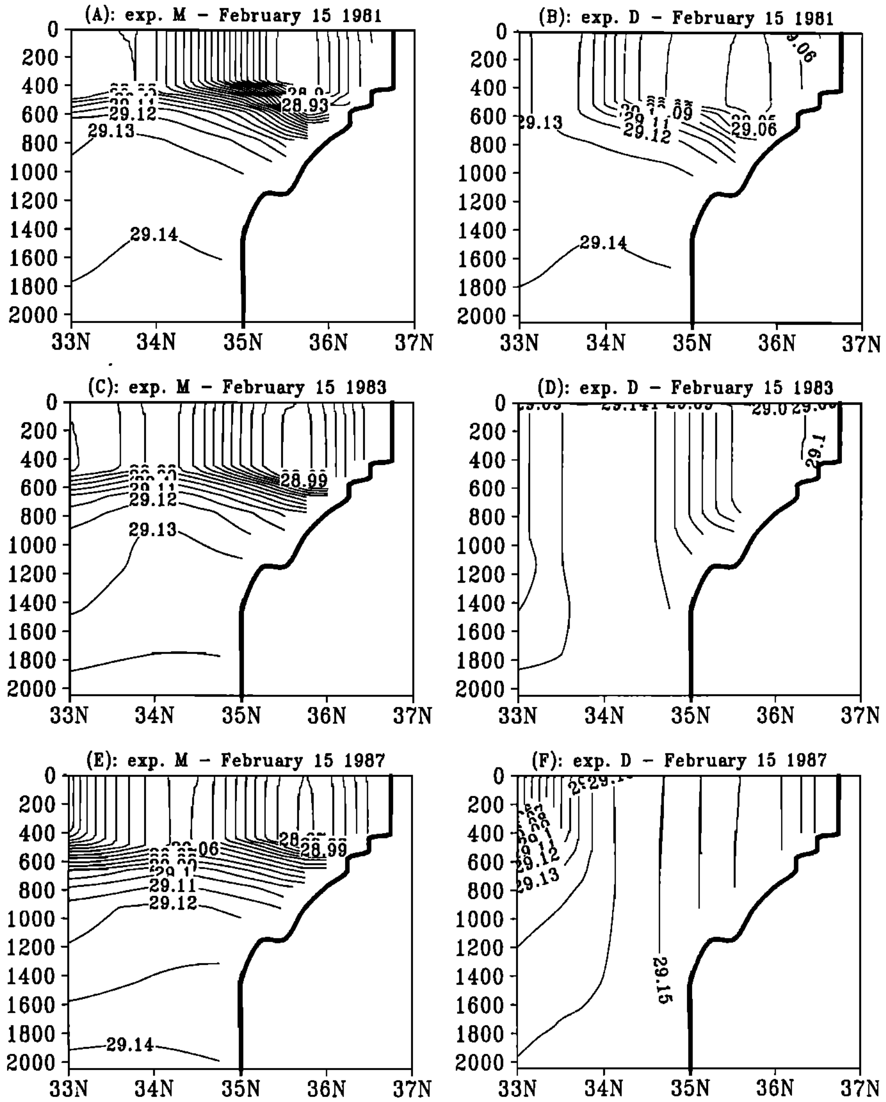


**Figure 6.** Density ($\sigma_T$, contour interval of 0.01) vertical section 3 (at Rhodes gyre) at 0-2050 m on February 15 for (a) year 1981 experiment M, (b) year 1981 experiment D, (c) year 1983 experiment M, (d) year 1983 experiment D, (e) year 1987 experiment M, and (f) year 1987 experiment D.

observed, and the outflow in the Ionian Basin occurs at a shallow depth (~ 1000 m). This may be again due to the absence of LIW in the subsurface. Furthermore, the model vertical and horizontal resolution in the deep levels prevent the correct dynamics of the bottom boundary layer from occurring and the right slantwise convection from being simulated [*Roether et al.*, 1994].

On the other hand, the D experiment shows strong deep convection in the southern Adriatic in all years (Table 10), again with the strongest events in 1981 and 1987 (Figures 8b, 8d, and 8f). The high-frequency forcing applied to the model definitely has the ability to enhance vertical mixing in the water column during the winter convection events, allowing newly formed water with $\sigma_T$ of about 29.10 - 29.14 and helping the outflow of the Strait of Otranto to reach depths of about 1700 m in the Ionian Basin. The temperatures are lower by about a degree than in the M experiment (Figure 10 a, 10c, and 10e), while the salinities keep the same values (Figures 10b, 10d, and 10f). The EMDW formation rates have been computed in the same way as for the LIW/LDW (Figure 11). This formation rate refers to the surface density of the mixed layer greater than 29.10 in the southern Adriatic area (area B in Figure 1). The M experiment (Figure 11a) produces EMDW only in 1987 (the strongest convection) and 1981, while the D experiment (Figure 11b) shows enhanced production of EMDW in 1981, 1984, 1985, and 1987. We interpret these results as indicative of the lower frequency of deep water formation than LIW/LDW, and we estimate an approximate 3-year frequency of formation.

### 4.5. Western Mediterranean Deep Water Formation

We examine a meridional cross section at 4.75°E cutting from 44°N to 40°N (section 1 in Figure 1) through

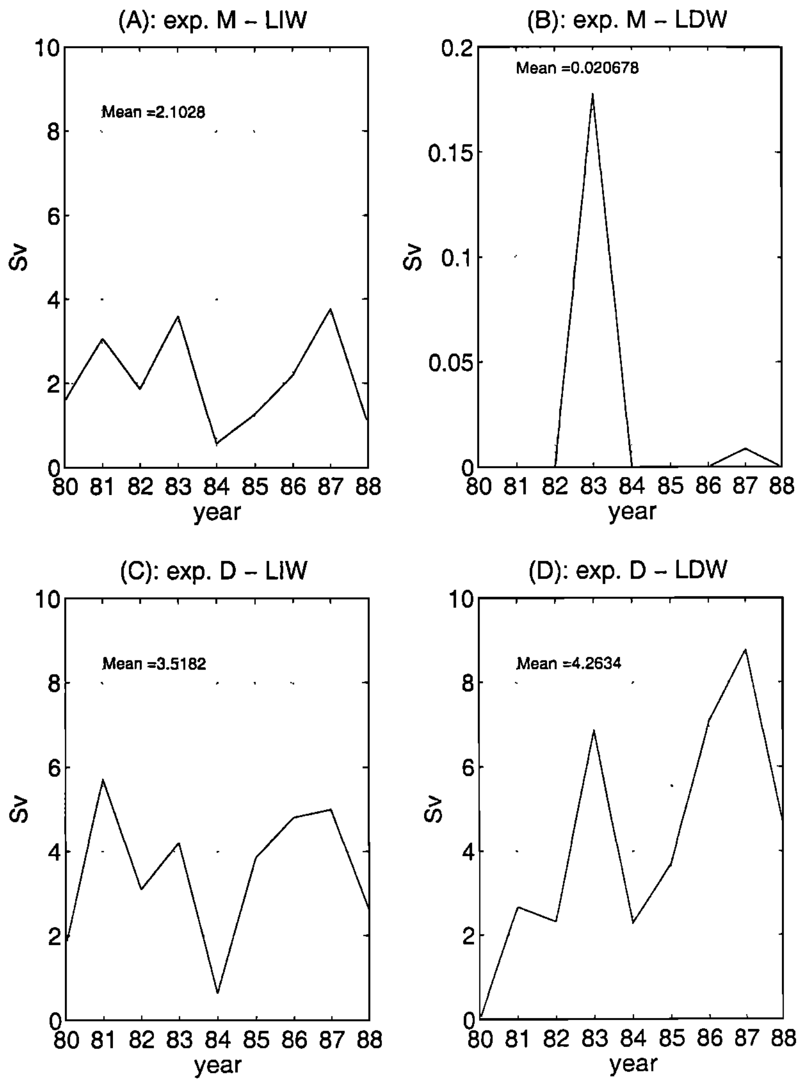


**Figure 7.** (a) Interannual variability of formation rate (Sv) of the LIW (28.95-29.10) for experiment M, (b) of LDW ($\geq$ 29.10) for experiment M, (c) LIW for experiment D, (e) and LDW for experiment D.

**Table 10.** Depth of Eastern Mediterranean Deep Water Outcropped Density Layers

| Year | M | D |
|---|---|---|
| 1980 | 600 m | d.c. |
| 1981 | d.c. | d.c. |
| 1982 | 600 m | d.c. |
| 1983 | 600 m | d.c. |
| 1984 | 600 m | d.c. |
| 1985 | 600 m | d.c. |
| 1986 | 600 m | d.c. |
| 1987 | d.c. | d.c. |
| 1988 | d.c. | d.c. |

Criterion is outcropping of layers with $\sigma_T$ between 29.10 and 29.20 for March of each year in southern Adriatic. The depth indicates where the deepest isopycnal of 29.10-29.20 is located before it outcrops. If deep convection (d.c.) takes place, then 29.10 and 29.20 are the bottom density layers.

an area (area A in Figure 1) where the preconditioning patch of surface water is present. We analyze first the preconditioning of the convection in December of each year (Figure 12 shows the preconditioning in years 1980, 1984, and 1986). In the M experiment the dome of the Lions gyre is well represented in all years, but the weakly stratified deep layer of WMDW already present in the area is less dense than climatological values (Figures 12a, 12c, and 12e). The intermediate layer of LIW present at 200-500 m is also less dense (28.75-28.95) due to an averaged salinity of 38.15-38.25 psu and an averaged temperature of 13.25°C (not shown here). While the LIW temperature is correct, the salinity is definitely lower compared to that observed in the preconditioning phase in December-January. The preconditioning problems shown by the M experiment are also present in the D experiment, but the latter shows a less stratified water column (Figures 12b, 12d, and 12f).

A criterion has been defined in this study in order to analyze WMDW formation; the outcropping of water

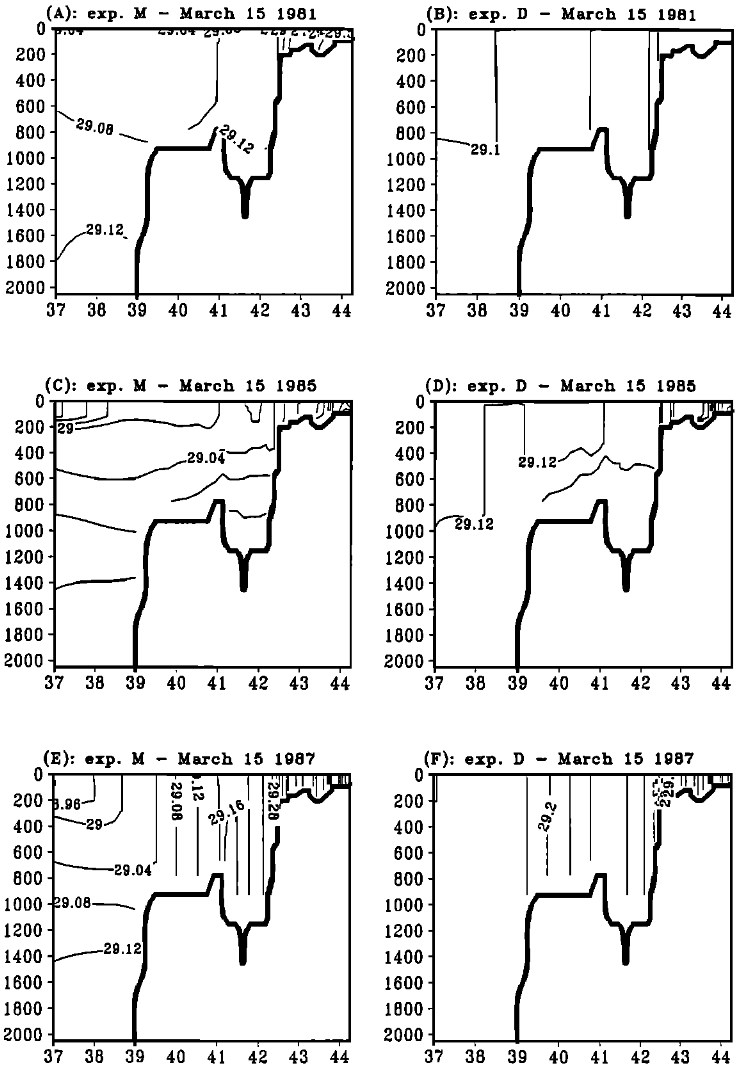


**Figure 8.** Density ($\sigma_T$, contour interval of 0.04) vertical section 2 (Adriatic-Ionian) at 0-2050 m on March 15 for (a) year 1981 experiment M, (b) year 1981 experiment D, (c) year 1985 experiment M, (d) year 1985 experiment D, (e) year 1987 experiment M, and (f) year 1987 experiment D.

layers with $\sigma_T$ between 29.00 and 29.15 during March on the meridional cross section in the convection area will indicate WMDW formation. Table 11 shows the results for deep water formation in March for the experiments M, MS, D, and DS listed in Table 5. March has been chosen as the typical month for the violent mixing phase, and in general all the numerical simulations show the convective process taking place starting from February and reaching maximum intensity in March.

Both the M and D experiments are unable to simulate the WMDW deep convection in any time of winter (Table 11). The D experiment (not shown here) produces mixed layer depths between 600 m and 800 m. The averaged mixed layer temperatures are around 13°C for the M experiment (not shown here) and around 12.3° - 12.5°C for the D experiment, while the averaged mixed layer salinities are the same for both experiments (around 38.05 - 38.15 psu). There is a drift toward lower mixed layer salinities, which is stronger in the D than in the M experiment.

The difficulty in simulating convection in area A has motivated new numerical experiments. Since the surface density is low compared to the density at deeper levels, the convective adjustment is unable to mix down to great depths, and this causes the deep water to form at shallower depths. In fact, all the model results show that the preconditioning phase is characterized by surface density values lower than those observed, so that when the violent mixing phase occurs, the deepening of the mixed layer stops at less dense levels. The low density values are mainly due to salinities lower than observed both at the surface and at the LIW levels.

We have then formulated the MS and DS experiments described in section 3 to increase salinity locally. The results of these new numerical experiments are shown in Figures 13-15. The mixed layer salinities of these

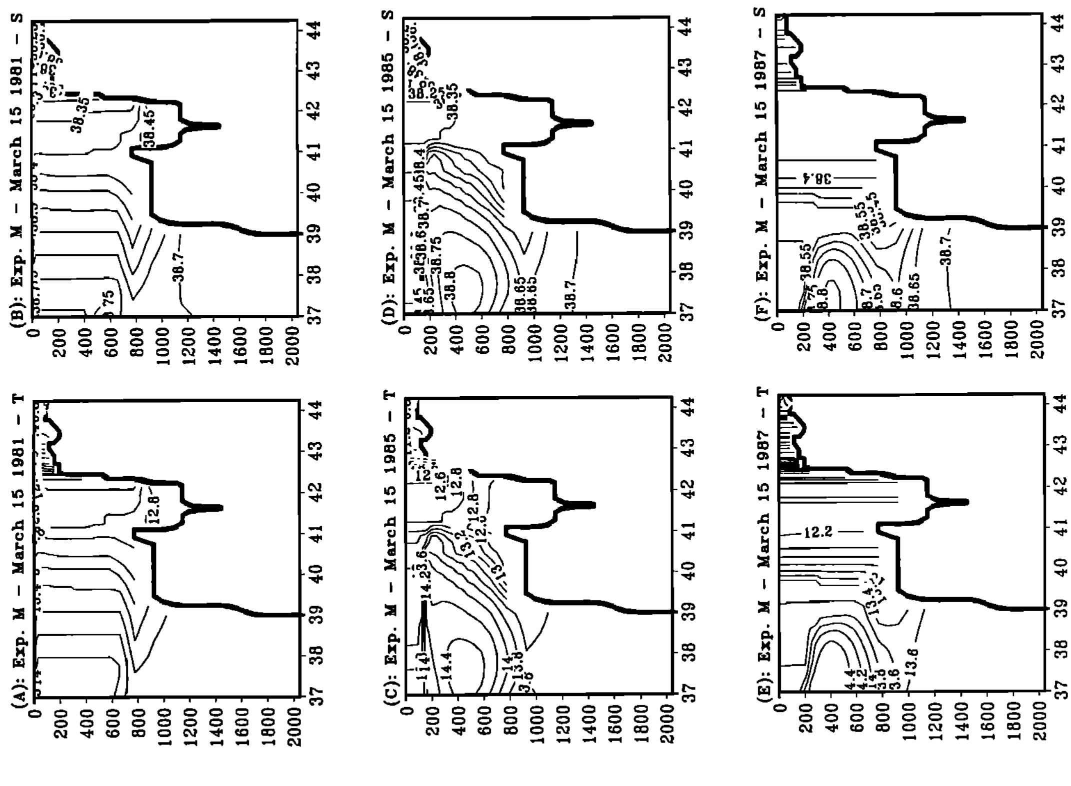


**Figure 9.** Experiment M: temperature (T, contour interval of 0.2° C) and salinity (S, contour interval of 0.05 psu) vertical section 2 (Adriatic-Ionian) at 0-2050 m on March 15 for (a, b) year 1981, (c, d) year 1985, and (e, f) year 1987.

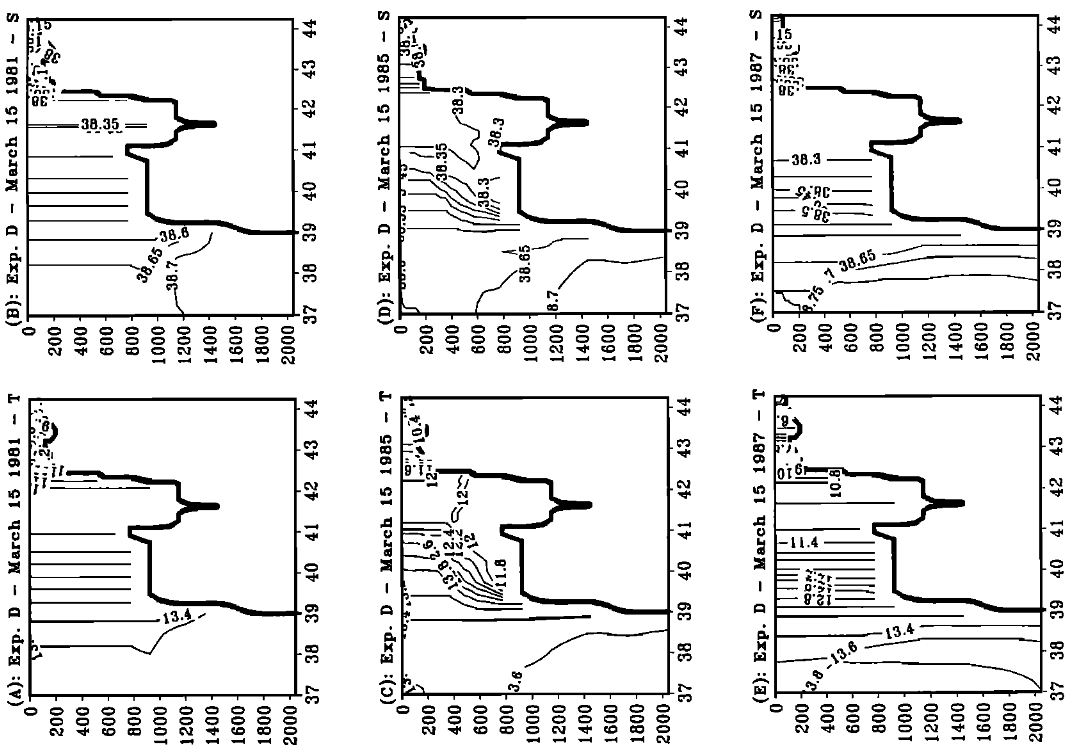


**Figure 10.** Experiment D: temperature (T, contour interval of 0.2° C) and salinity (S, contour interval of 0.05 psu) vertical section 2 (Adriatic-Ionian) at 0-2050 m on March 15 for (a, b) year 1981, (c, d) year 1985, and (e, f) year 1987.

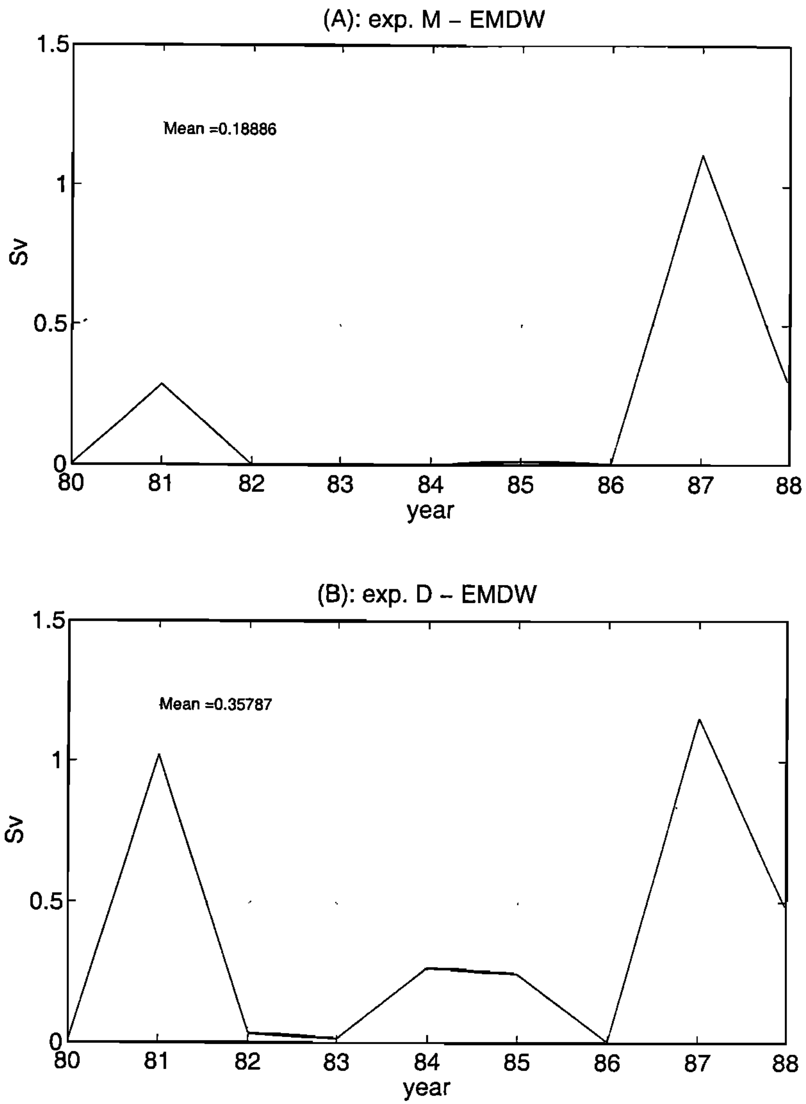


**Figure 11.** Interannual variability of formation rate (Sv) of the EMDW ($\geq$ 29.10) (Adriatic Deep Water) component: (a) experiement M and (b) experiment D.

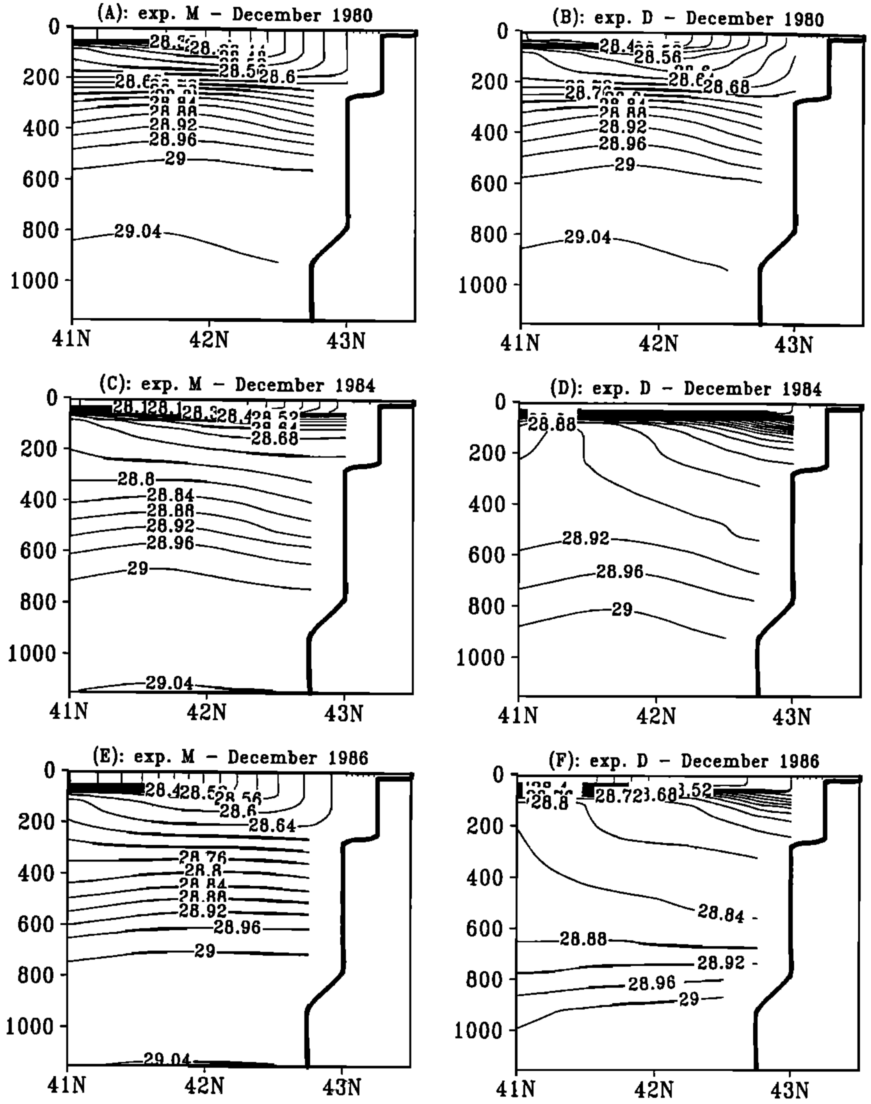


**Figure 12.** December monthly mean density ($\sigma_T$, contour interval of 0.04) vertical section 1 (Gulf of Lions) at 0-1150 m for (a) year 1980 experiment M, (b) year 1980 experiment D, (c) year 1984 experiment M, (d) year 1984 experiment D, (e) year 1986 experiment M, and (f) year 1986 experiment D.

**Table 11.** Depth of Western Mediterranean Deep Water Formation for Experiments M, D, MS, and DS

| Year | M | D | MS | DS |
|---|---|---|---|---|
| 1980 | no | no | no | ~ 400 m |
| 1981 | no | ~ 500 m | ~ 700 m | ~ 800 m |
| 1982 | no | no | ~ 500 m | ~ 700 m |
| 1983 | no | ~ 400 m | ~ 600 m | o.d.c. |
| 1984 | no | ~ 600 m | no | o.d.c. |
| 1985 | no | ~ 600 m | no | ~ 800 m |
| 1986 | no | ~ 700 m | no | s.d.c. |
| 1987 | ~ 500 m | ~ 800 m | no | o.d.c. |
| 1988 | ~ 600 m | ~ 600 m | no | ~ 900 m |

Criterion is outcropping of layèra of $\sigma_T$ between 29.00 and 29.15 for March of each year. The depth indicates where the deepest isopycnal of 29.00-29.15 is located before it outcrops. Open ocean deep convection is indicated by o.d.c. and shallow water convection on the shelf area near the Gulf of Lions area is indicated by s.d.c.

new experiments are larger by about 0.3 psu than the salinities of the M and D experiments (Figure 13 and Figure 14). The stratification of the water column is strongly reduced, and deeper convection events occur in area A with low-frequency forcing, and full convection occurs with the high-frequency forcing. Full deep convection is produced with the correct density of the deep water ($\sigma_T$ = 29.06 in March 1987) in the DS experiment during the years 1983, 1984, 1986, and 1987 (Figure 15 b, 15d, and 15f). In Table 11 we show that only DS is capable of producing deep ocean convection processes both in the open ocean area and in shelf areas.

It is interesting to analyze the volume of LIW present in area A in the month of January of each year for each numerical experiment. The LIW volume has been defined by salinities ranging between 38.45 psu and 38.75 psu at depths of 400-800 m. This LIW volume gives an indication of the preconditioning state of the the water layers present in area A for possible deep convec-

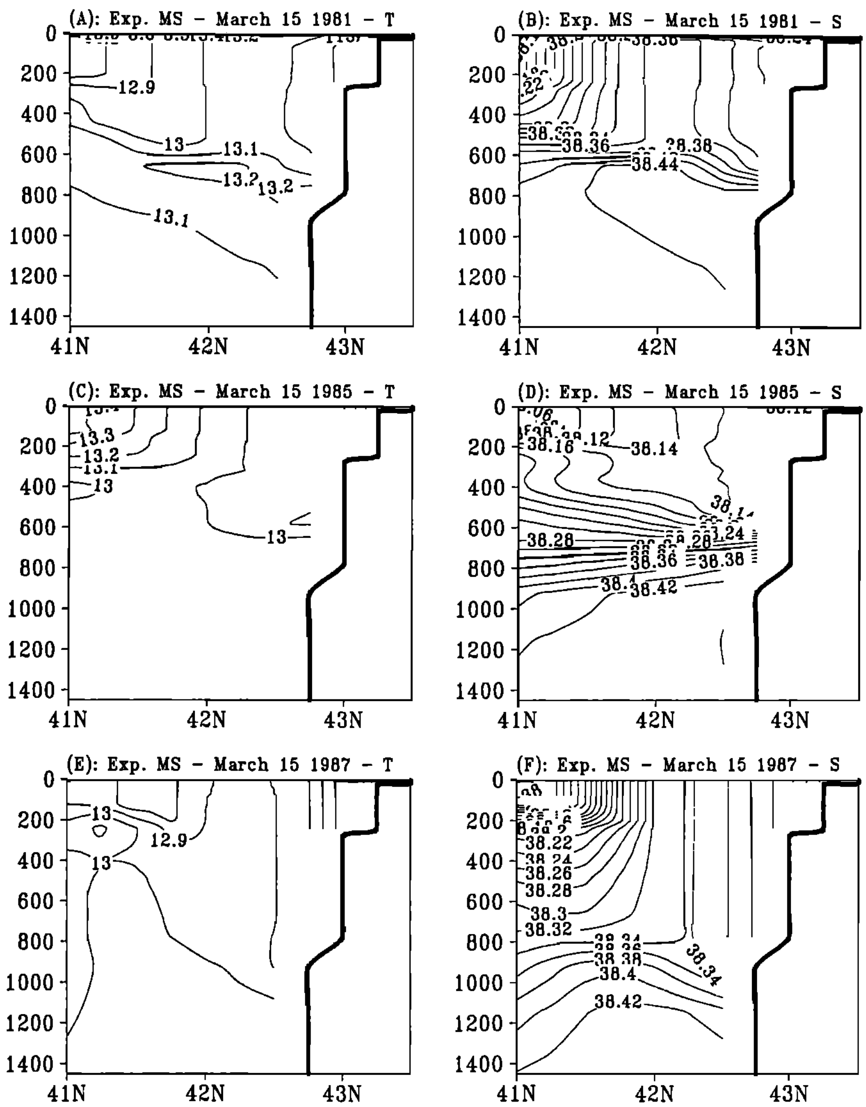


**Figure 13.** Experiment MS: temperature (T, contour interval of 0.1° C) and salinity (S, contour interval of 0.02 psu) vertical section 1 (Gulf of Lions) at 0-1450 m on March 15 for (a, b) year 1981, (c, d) year 1985, and (e, f) year 1987.

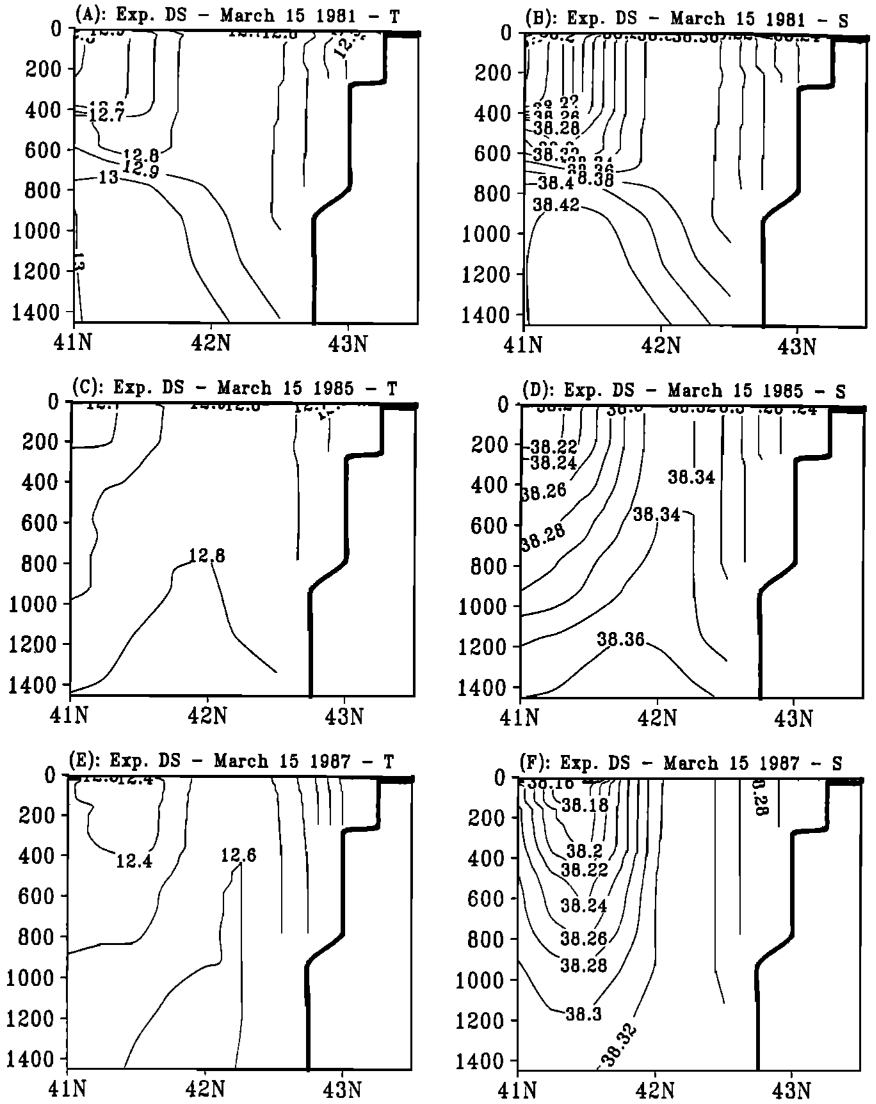


**Figure 14.** Experiment DS: temperature (T, contour interval of 0.1° C) and salinity (S, contour interval of 0.02 psu) vertical section 1 (Gulf of Lions) at 0-1450 m on March 15 for (a, b) year 1981, (c, d) year 1985, and (e, f) year 1987.

tion events. Table 12 shows that the experiments with the 12-hour forcing (D and DS) lose the LIW layer more rapidly than the other experiments. This indicates that the high-frequency forcing applied in the model tends to diffuse or mix the pycnocline too strongly, thus producing a well-mixed preconditioned water column.

The WMDW yearly formation rate in sverdrups is estimated with the same method as LIW/LDW and EMDW by computing the maximum volume of WMDW with $\sigma_T$ between 29.00-29.15 present in the mixed layer over area A and dividing by 1 year. In this case the assumption of nonpenetrative convection can be too approximate for the application to the WMDW formation process, but is quite justified for its simplicity. The M and MS experiments show low production rates of WMDW, while the DS experiment gives appreciable formation rates (Figure 16). The average value from the DS experiment is around 1.6 Sv, which is comparable with the estimated value of 1.0 Sv by *Tziperman and Speer* [1994]. These rates show the largest values in 1981, 1984, and 1987, two of them (1981 and 1987) years of intense winter, with strong momentum and heat forcing in the overall basin as found by *Mertens and Schott* [1998]. The WMDW interannual variability in formation rates has approximately a period of 3 years as for the EMDW and LDW formation processes.

## 5. Sensitivity experiments

The high average formation rates of LIW and LDW and the lower temperature values of all our water masses have prompted us to change the air-sea interaction physics in order to decrease the amount of heat loss at the surface. Two experiments have been designed with (1) $Q_B$ estimated by the Brunt-Berliand formula (the DS1 experiment) and (2) $Q_B$ estimated by the Berliand-Berliand formula (the DS2 experiment). These two different bulk formulae have been shown by *Castellari et*

**Table 12.** Volume of LIW (38.45 $\leq$ S $\leq$ 38.75) at 400 - 800 m Depths in area A in January (monthly mean)

| Year | M | MS | D | DS |
|---|---|---|---|---|
| 1980 | 25 | 25 | 25 | 25 |
| 1981 | 34 | 31 | 32 | 27 |
| 1982 | 42 | 24 | 12 | 44 |
| 1983 | 38 | 14 | 81 | 15 |
| 1984 | 33 | 10 | 20 | 0 |
| 1985 | 32 | 80 | 0 | 0 |
| 1986 | 31 | 56 | 0 | 0 |
| 1987 | 30 | 27 | 0 | 0 |
| 1988 | 17 | 93 | 0 | 0 |

Values are in $10^3$ km$^3$.

*al.*, [1998] to produce a lower long-term net heat budget. We have estimated the formation rates and the surface integral of the heat budgets as done previously for the past experiments. The formation rates of the DS2 experiment are shown in Figure 17 and of the DS1 experiment in Figure 18. Concerning the LIW/LDW, we see that the DS2 experiment presents a value of 2.2 Sv for LIW and 2.7 Sv for LDW (Figures 17a, and 17b) and a heat budget of about -5.3 W/m $^2$. LDW production is more sporadic in time than the LIW production, with large peaks in 1983 and 1987 as for the DS experiment. On the other hand, the DS1 experiment has reduced the LIW production to a very realistic value of 1.5 Sv and LDW to 0.9 Sv (Figures 18a, and 18b), but the overall heat budget is positive (about 1 W/m $^2$) and it does not produce as much WMDW and EMDW as

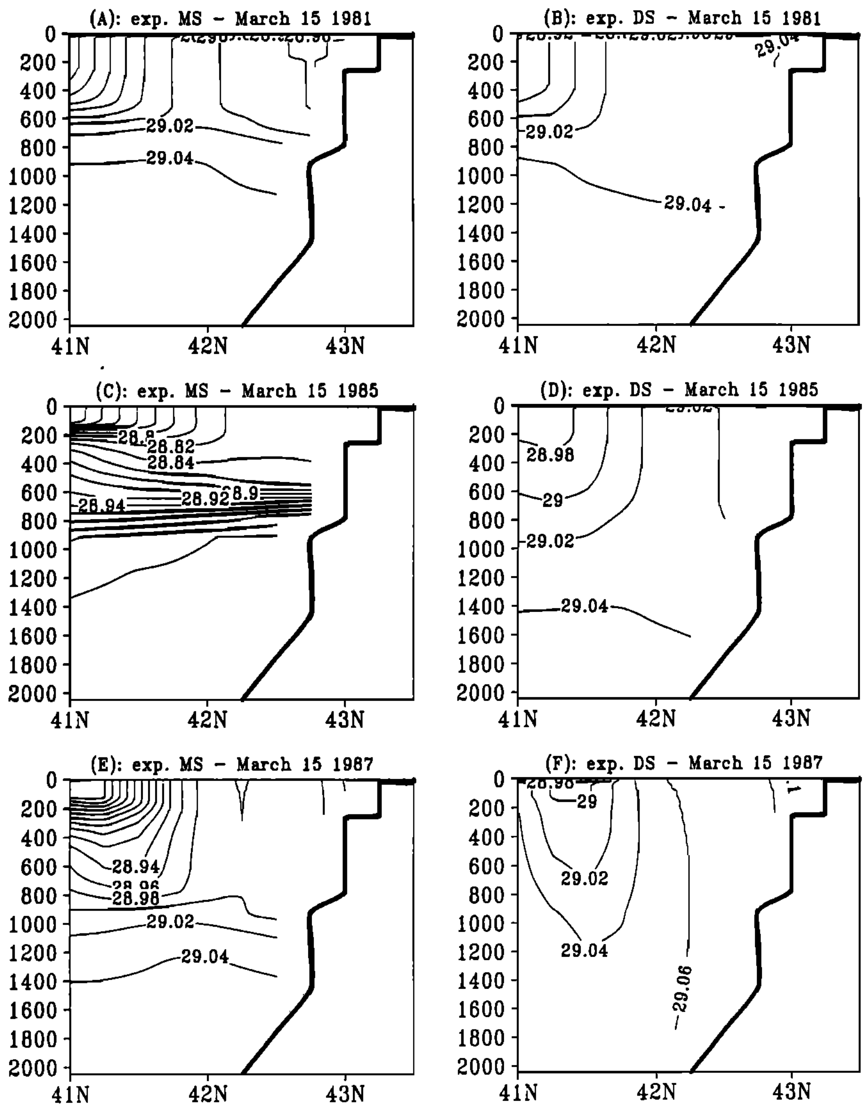


**Figure 15.** Density ($\sigma_T$, contour interval of 0.02) vertical section 1 (Gulf of Lions) at 0-2050 m on March 15 for (a) year 1981 experiment MS, (b) year 1981 experiment DS, (c) year 1985 experiment MS, (d) year 1985 experiment DS, (e) year 1987 experiment MS, and (f) year 1987 experiment DS.

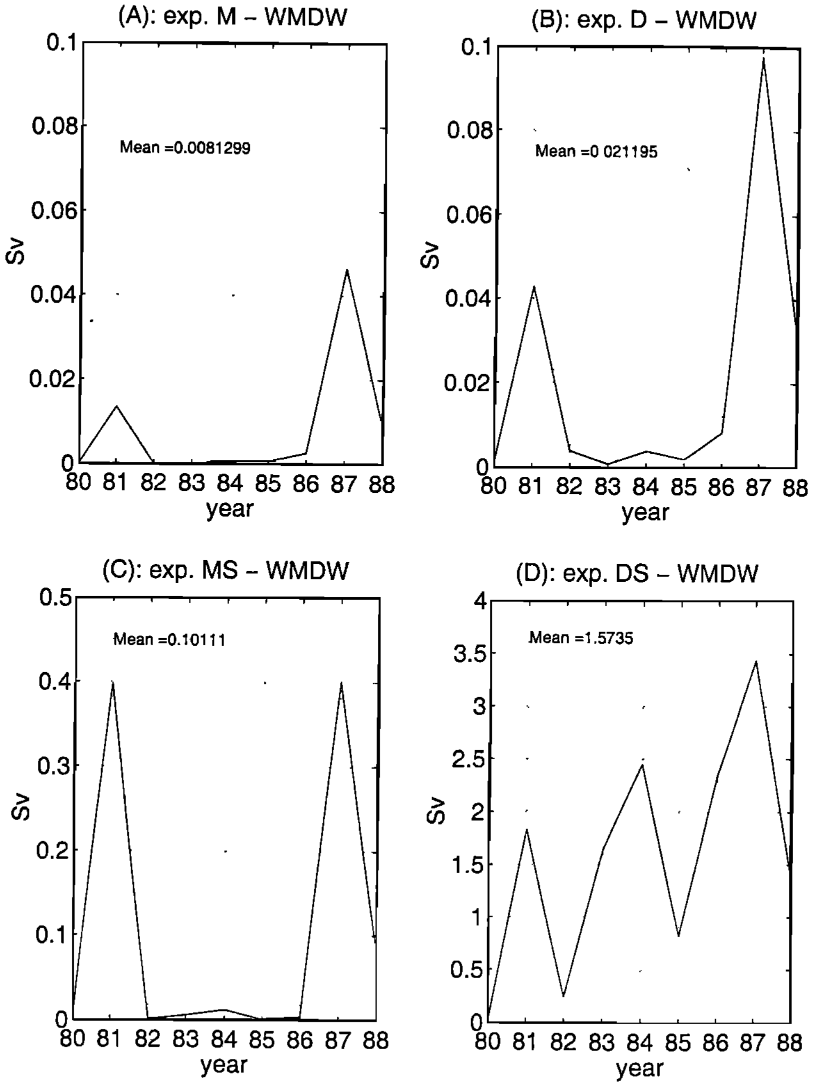


**Figure 16.** Interannual variability of formation rate (Sv) of the WMDW (29.00-29.15): (a) experiment M, (b) experiment D, (c) experiment MS, and (d) experiment DS.

known to occur (Figures 18c, and 18d). The DS1 experiment clearly has a larger climate drift than the other DS experiments, due to the positive long-term surface heat budget which affects mainly the deep water masses of the basin. We believe that within the limitation of our modeling approach, LIW can be considered to form at a realistic rate and the annual frequency is confirmed. Both DS1 and DS2 experiments have shown an EMDW formation rate of about 0.3 Sv with an approximate 3-year frequency (Figures 17c, and 18c) as found in the DS experiment. The WMDW formation rate produced from the DS2 experiment is around 1.1 Sv (comparable to the value of the DS experiment), while that one of the DS1 experiment is around 0.2 Sv. This shows that WMDW is more sensitive to the overall heat budgets than LIW, LDW, and EMDW.

## 6. Conclusions

The goal of this study is to gain insight into the interannual variability of water mass formation processes of the Mediterranean Sea by analyzing the response of the MEDMOM to different atmospheric forcing frequencies for the period 1980-1988 (monthly mean and 12-hour).

Each different water mass formation process for LIW, LDW, EMDW (only the ADW component), and WMDW is investigated as a function of different atmospheric frequency forcings with a particular emphasis on the WMDW convection. The M experiments simulate quite well the LIW shallow convection, while the D experiments produce mostly Levantine deep convection (LDW) due to large heat losses occurring in the area of formation. In both experiments the temperature and salinity values of the newly formed water are consistently lower than the climatologically observed LIW values, indicating that the simulated convection is mainly triggered by cooling rather than salinity effects. Only the temperatures of the LDW produced with the D experiment are in agreement with *Gertman et al.*, [1994]. The LIW formation rates show strong interannual fluctuations but with a tendency to take place every year.

By analyzing the EMDW formation, both the M and D experiments produce convective events in the southern Adriatic in 1981 and 1987, and shallower convection in the other years. The high-frequency forcing has the ability to enhance vertical mixing in the water column, allowing newly formed water with $\sigma_T$ of 29.10 or more to flow out from the Strait of Otranto. The frequency of water formation estimated from these experiments is 3 years for a conservative estimate, but it can be as long as 6 years if we consider the M experiments.

In the Gulf of Lions area the M and D experiments simulate well the doming of the Lions gyre during the preconditioning phase, but during the violent mixing phase the vertical sections show mostly shallow convection with outcropping only of the 28.85-28.95 isopycnals.

The difficulty in simulating the correct deep convection in the Lions gyre has motivated new numerical experiments with salinity enhancement. To improve this situation, the surface density in the area of the convective patch is increased through a SSS correction applied to the salinity vertical boundary condition (MS and DS experiments). With this correction, only the experiment using the 12-hour forcing is able to produce deep convection approximately every 3 years and in particular the outcropping of the 29.05 density surface in the Gulf of Lions during March 1987. This is the same year when *Leaman and Schott* [1991] found observational evidence of deep convection occurring in mid-January and around the last week of February with a WMDW density of about 29.10.

The high formation rate of LIW and LDW obtained in the DS experiment forced us to use different air-sea interaction physics to try to lower the net formation rate. This was achieved in the DS2 experiment, which showed the same water mass formation variability but more realistic long-term average formation rates. Relevant deep water formation processes occur sporadically

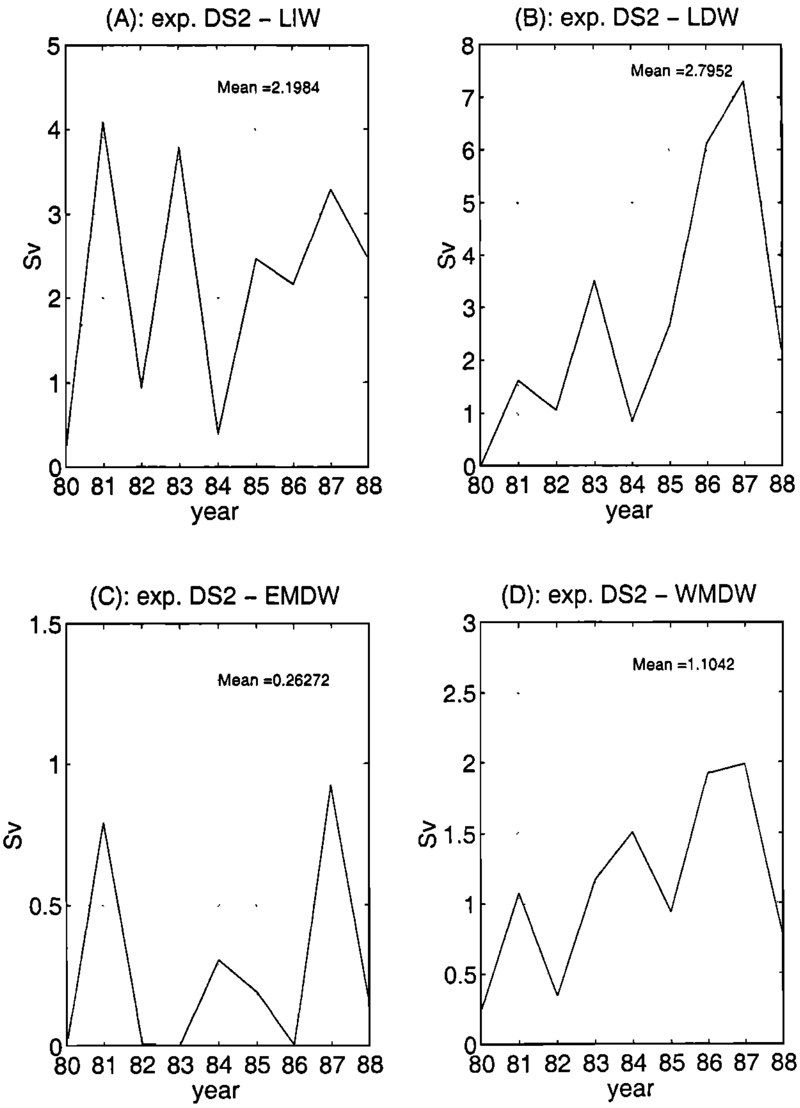


**Figure 17.** Interannual variability of formation rate (Sv) for experiment DS2 of (a) LIW (28.95-29.10), LDW ($\geq$ 29.10), EMDW ($\geq$ 29.10) (ADW component), and (d) WMDW (29.00-29.15).

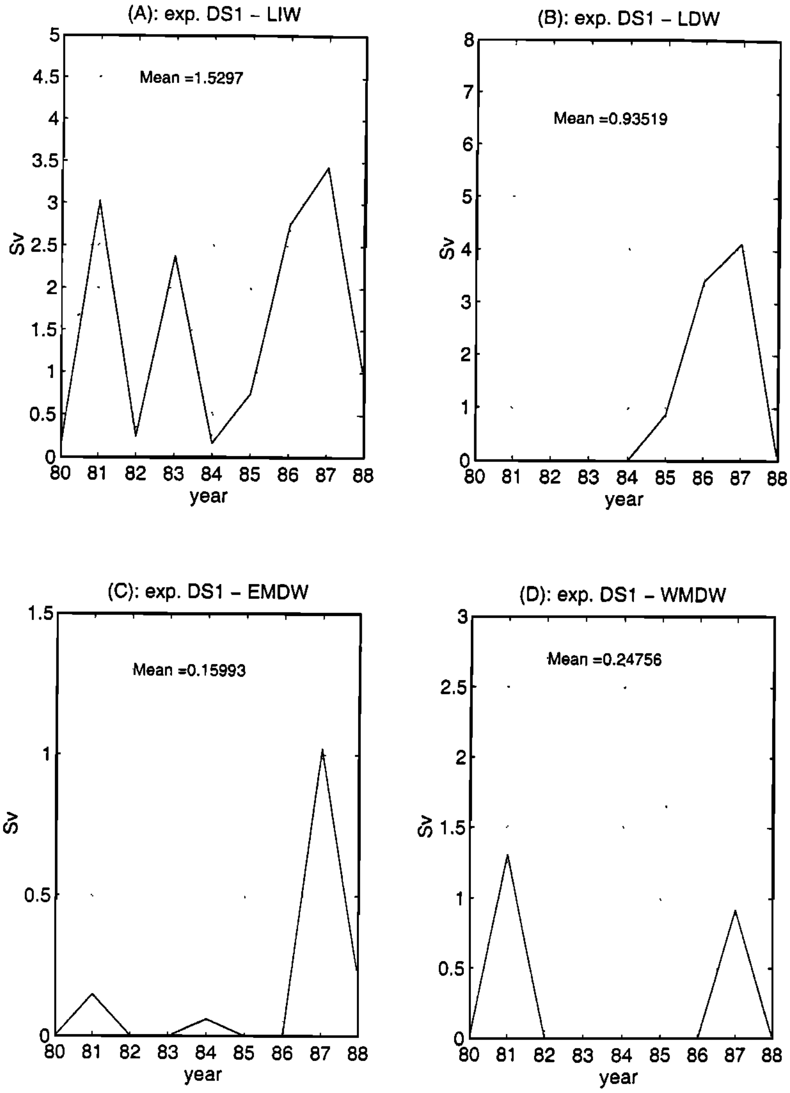


**Figure 18.** Interannual variability of formation rate (Sv) for experiment DS1 of (a) LIW (28.95-29.10), (b) LDW ($\geq$ 29.10), (c) EMDW ($\geq$ 29.10) (ADW component), and (d) WMDW (29.00-29.15).

with a 2-3 year frequency, but the too short duration of our experiments does not allow us to be definitive on the periodicity. Moreover, it is concluded that deep water mass formation occurs following, but not necessarily limited by, anomalous wind forcing events. In fact, in 1984, with a winter event of moderate amplitude, WMDW is still produced. Thus the oceanic response to atmospheric forcing for deep water masses is highly nonlinear and depends on different preconditioning: 1981 and 1987 are overall two years of intense LIW, LDW, EMDW, and WMDW formation events, whereas 1983 and 1984 are more sensitive to model setup.

## Notation

| | |
|---|---|
| $\mathbf{u}$ | full three dimensional velocity vector. |
| $\mathbf{u_h}$ | horizontal component of $\mathbf{u}$. |
| $\mathbf{f} = \mathbf{k}\, f$ | Coriolis vector. |
| $f = 2\,\Omega \sin(\theta)$ | Coriolis vector magnitude. |
| $\mathbf{k}$ | unit vector in the z direction. |
| $p$ | pressure. |
| $\rho$ | density. |
| $g$ | mean gravity. |
| $T$ | temperature. |
| $S$ | salinity. |
| $T^*$ | known climatological temperature. |
| $S^*$ | known climatological salinity. |
| $\alpha_T$ | temperature Newtonian restoring term. |
| $\alpha_S$ | salinity Newtonian restoring term. |
| $A_M$ | horizontal eddy viscosity. |
| $A_T$ | horizontal eddy diffusivity. |
| $K_M$ | vertical eddy viscosity. |
| $K_T$ | vertical eddy diffusivity. |

**Acknowledgments.** We would like to thank A. Rosati (GFDL-NOAA, Princeton, New Jersey) and A. Oort (GFDL-

NOAA, Princeton, New Jersey), who have given us the NCEP data and the COADS data. We appreciate also the valuable assistance provided by G. Korres (Athens University, Greece), A. Navarra (ING, Roma, Italy), Jean Carpenter (RSMAS, University of Miami, Florida), P. Carini and E. Masetti (ISAO-CNR, Bologna, Italy). We also thank L. Amato (ISAO-CNR, Bologna, Italy) for her helpful editorial assistance. This research has been partially undertaken within the framework of the Mediterranean Targeted Project (MTP) phase II-MATER (publication MTP II-MATER/020). We acknowledge the support from the European Commission's Marine Science and Technology Programme (MAST III) under contract MAS3-CT96-0051 and from the National Science Foundation (NSF-USA) (grant OCE-91 15995). We also thank two anonymous reviewers for their helpful comments.

## References

Artegiani, A., R. Azzolini, and E. Salusti, On the dense water in the Adriatic Sea, *Oceanol. Acta, 12,* 151-160, 1989.

Artegiani, A., D. Bregant, E. Paschini, N. Pinardi, F. Raicich, and A. Russo, The Adriatic general circulation. Part 1: air sea interaction and water mass structure, *J. Phys. Oceanogr., 27,* 1492-1514, 1997.

Berliand, M.E., and T.G. Berliand, Determining the net long-wave radiation of the earth with consideration of the effect of cloudiness, *Isv. Akad. Nauk. SSSR Ser. Geofis., 1,* 1952.

Bethoux, J.P., Budgets of the Mediterranean Sea: their dependence on the local climate and on the characteristics of the Atlantic waters, *Oceanol. Acta, 2,* 157-163, 1979.

Brasseur, P., J.M. Beckers, J.M. Brankart, and R. Schoenauen, Seasonal temperature and salinity fields in the Mediterranean Sea: Climatological analyses of an historical data set, *Deep Sea Res. 43*(2), 159-192, 1996.

Bryan, K., A numerical model for the study of the world ocean, *J. Comput. Phys., 4,* 347-376, 1969.

Budyko, M.I., *Climate and Life,* 508 pp., Academic, San Diego, Calif., 1974.

Bunker, A.F., H. Charnock, and R.A. Goldsmith, A note on the heat balance of the Mediterranean and Red Seas, *J. Mar. Res., 40,* Suppl., 73-84, 1982.

Castellari, S., A numerical study of water mass formation processes and seasonal to interannual variability in the Mediterranean Sea, Univ. of Miami, Miami, Fla., USA, Ph.D. dissertation, Rosenstiel Sch. of Mar. and Atmos. Sci., 1996.

Castellari, S., N. Pinardi, and K.D. Leaman, A model study of air-sea interactions in the Mediterranean Sea, *J. Mar. Syst., 18,* 89-114, 1998.

Cox, M.D., A primitive equation, 3-dimensional model of the ocean. *GFDL Ocean Group Tech. Rep. 1,* 143 pp., Geophys. Fluid Dyn. Lab., Princeton, N.J., 1984.

Garrett, C., R. Outerbridge, and K. Thompson, Interrannual variability in Mediterranean Heat and Buoyancy Fluxes, *J. Clim., 6,* 900-910, 1993.

Gertman, I.F., Y.I. Popov, and V.G. Trigub, Deep convection in the Levantine Sea, March 1987, Viniti, Moscow, *Rep. 6581-B87,* 1987.

Gertman, I.F., I.M. Ovchinnikov, and Yu.I. Popov, Deep convection in the eastern basin of the Mediterranean Sea, *Oceanology, 34,* (1), 19-24, 1994.

Gilman, C., and C. Garrett, Heat flux parameterizations for the Mediterranean Sea: The role of atmospheric aerosols and constraints from the water budget, *J. Geophys. Res., 99,* 5119-5134, 1994.

Haines, K., and P. Wu, A modelling study of the thermohaline circulation of the Mediterranean: water formation and dispersal. *Oceanol. Acta, 18,* 401-417, 1995.

Haney, R.L., Midlatitude sea surface temperature anomalies: a numerical hindcast. *J. Phys. Oceanogr., 15,* 787-799, 1985.

Hecht, A.N., The hydrology and the water masses of the eastern Mediterranean Sea, in *Proceedings of UNESCO/I OC First POEM Workshop, Erdemli-Icel, Turkey, 1986,* Part2, *POEM Sci. Rep. 1,* edited by A.R. Robinson and P.M. Rizzoli, p.51, Harvard Univ., Cambridge, Mass., 1986.

Hecht, A., N. Pinardi and A. Robinson, Current, water masses, eddies and jets in the Mediterranean Levantine basin, *J. Phys. Oceanogr., 18,* 1320-1353, 1988.

Hellerman, S., and M. Rosenstein, Normal monthly wind stress over the world ocean with error estimates, *J. Phys. Oceanogr., 13,* 1093-1104, 1983.

Jones, H., and J. Marshall, Convection with rotation in a neutral ocean; a study of open-ocean deep convection, *J. Phys. Oceanogr., 23,* 1009-1039, 1993.

Kondo, J., Air-sea bulk transfer coefficients in diabatic conditions, *Boundary Layer Meteorol., 9,* 91-112, 1975.

Korres, G., and N. Pinardi, and A. Lascaratos, The ocean response to low frequency interannual atmospheric variability in the Mediterranean sea. Part I: Sensitivity experiments and energy analysis, *J. Clim., 13,* 705-731, 2000.

Lacombe, H., and P. Tchernia, Caracters hydrologiques et circulation des eaux en Mediterranee, in *The Mediterranean Sea: A Natural Sedimentation Laboratory,* edited by D.J. Stanley, pp. 25-36, Dowden, Hutchinson and Ross, Stroudsburg, Pa., 1972.

Lascaratos, A., R.G. Williams, and E. Tragou, A mixed-layer study of the formation of Levantine Intermediate Water, *J. Geophys. Res., 98,* 14,739-14,749, 1993.

Leaman, K.D., and F.A. Schott, Hydrographic structure of the convection regime in the Gulf of Lions: winter 1987, *J. Phys. Oceanogr., 21,* 575-598, 1991.

Legg, S., and J. Marshall, A heton model of the spreading phase of open-ocean deep phase of open-ocean deep convection, *J. Phys. Oceanogr., 23,* 1041-1056, 1993.

Macdonald, A., J. Candela, and H.L. Bryden, An estimate of the net heat transport through the Strait of Gibraltar, in *Seasonal and Interannual Variability of the Western Mediterranean Sea,* edited by P.E. La Violette, *Coastal Estuarine Sci. Ser.,* vol. 46, AGU, Washington, D.C., 1994.

Madec, G., M. Chartier, and M. Crepon, The effect of thermohaline forcing variability on deep water formation in the western Mediterranean Sea: A high resolution three-dimensional numerical study, *Dyn. Atmos. Oceans, 15,* 301-332, 1991a.

Madec, G., M. Chartier, P. Delecluse, and M. Crepon, A three-dimensional numerical study of deep-water formation in the Northwestern Mediterranean Sea, *J. Phys. Oceanogr., 21,* 1349-1371, 1991b.

May, P.W., A brief explanation of Mediterranean heat and momentum flux calculations, *NORDA Rep. 322,* Naval Oceanogr. and Atmos. Res. Lab., Stennis Space Center, Miss., 1986.

MEDOC Group, Observation of formation of deep water in the Mediterranean Sea, *Nature, 227,* 1037-1040, 1970.

Mertens, C., and Schott F., Interannual variability of deep-water formation in the Northwestern Mediterranean, *J. Phys. Oceanogr., 28,* 1410-1424, 1998.

Nittis, K., and A. Lascaratos, Diagnostic and prognostic numerical studies of LIW formation, *J. Mar. Syst., 18,* 179-195, 1998.

Ovchinnikov, I.M., The renewal of the principal water masses of the Mediterranean, *Oceanology, 23,* 719-721, 1983.

Ovchinnikov, I.M., The formation of intermediate water in the Mediterranean Sea, *Oceanology, 24,* 168-173, 1984.

Ovchinnikov, I.M., V.I. Zats, V.G. Krivosheya, M.S. Nemirovsky, and A.I. Udodov, Winter convection in the Adriatic and formation of deep eastern Mediterranean waters, *Ann. Geophys., 5B,* 89-92, 1987.

Ozsoy, E., A. Hecht, and U. Unluata, Circulation and hydrography of the Levantine Basin: Results of POEM Coordinated Experiments 1985-1986, *Prog. Oceanogr., 22,* 125-170, 1989.

Ozsoy, E., A. Hecht, U. Unluata, S. Brenner, H.I. Sur, J. Bishop, M.A. Latif, Z. Rozentraub, and T. Oguz, A synthesis of the Levantine basin circulation and hydrography, 1985-1990, *Deep Sea Res., Part II, 40,* 1075-1119, 1993.

Ozturgut, E., The source and spreading of the Levantine Intermediate Water in the eastern Mediterranean, *Memo. SM-92,* Saclant ASW Res. Cent., 45 pp., La Spezia, Italy, 1976.

Pacanowski, R.C., K. Dixon, and A. Rosati, README file for GFDL MOM 1.0, Geophys. Fluid Dyn. Lab., Princeton, N.J., 1991.

Peixoto, J., M. De Almeida, R. Rosen, and D. Salstein, Atmospheric moisture transport and the water balance of the Mediterranean Sea, *Water Resour. Res., 18,* 83-90, 1982.

Pinardi, N., G. Korres, A. Lascaratos, V. Roussenov, and E. Stanev, Numerical simulation of the interannual variability of the Mediterranean Sea upper ocean circulation, *Geophys. Res. Lett., 24,* 425-428, 1997.

Plakhin, A., and V.G. Smirnov, On the determination of initial *T,S* indices of the Mediterranean Sea waters, *Oceanology, 24,* 174-177, 1984.

Pollak, M.I., The sources of deep water of the eastern Mediterranean Sea, *J. Mar. Res., 10,* 128-152, 1951.

Reed, R.K., On estimating insolation over the ocean, *Prog. Oceanogr., 17,* 854-871, 1977.

Reynolds, R.W., A real-time global sea surface temperature analysis, *J. Clim., 1,* 75-86, 1988.

Robinson, A.R., M. Golnaraghi, W.G. Leslie, A. Artegiani, A. Hecht, E. Lazzoni, A. Michelato, E. Sansone, A. Theocharis, and U. Unluata, The eastern Mediterranean general circulation: features, structure and variability, *Dyn. Atmos. Oceans, 15,* 215-240, 1991.

Roether, W., V. Roussenov, and R. Well, A tracer study of the thermohaline circulation of the eastern Mediterranean, in *Ocean Processes in Climate Dynamics,* edited by P.M. Rizzoli and A. Robinson, pp. 371-394, Kluwer, Norwell, Mass., 1994.

Roether, W., B. Manca, D. Klein, D. Bregant, D. Georgopoulos, W. Beitzel, V. Kovacevic, and A. Luchetta, A., Recent changes in Eastern Mediterranean Deep Waters, *Science, 271,* 333-334, 1996.

Rohling, E.J., and H.L. Bryden, Man-induced salinity and temperature increases in the Western Mediterranean deep water, *J. Geophys. Res., 97,* 11,191-11,198, 1992.

Roussenov, V., E. Stanev, V. Artale, and N. Pinardi, A seasonal model of the Mediterranean Sea circulation, *J. Geophys. Res., 100,* 13,515-13,538, 1995.

Schott, F., and K.D. Leaman, Observations with moored acoustic Doppler current profilers in the convection regime in the Golfe of Lion, *J. Phys. Oceanogr., 21,* 558-574, 1991.

Schott, F., M Visbeck, and U. Send, Open-ocean deep convection, Mediterranean and Greenland Seas, in *Ocean Processes on Climate Dynamics,* edited by P.M. Rizzoli and A. Robinson, pp. 203-225, Kluwer, Norwell, Mass., 1994.

Schott, F., M. Visbeck, U. Send, J. Fischer, L. Stramma, and Y. Desaubies, Observations of deep convection in the Gulf of Lions, northern Mediterranean, during the winter of 1991/92, *J. Phys. Oceanogr., 26,* 505-524, 1996.

Send, U., and J. Marshall, Integral effects of deep convection, *J. Phys. Oceanogr., 25,* 855-872, 1995.

Send, U., F. Schott, F. Gaillard, and Y. Desaubies, Observation of a deep convection regime with acoustic tomography, *J. Geophys. Res., 100,* 6927-6941, 1995.

Stommel, H., Deep winter-time convection in the western Mediterranean Sea, in *Studies in Physical Oceanography,* v. 2, edited by A.L. Gordon, pp. 207-218, Gordon and Breach, Newark, N.J., 1972.

Tziperman, E., and K. Speer, A study of water mass transformation in the Mediterranean Sea: Analysis of climatological data and a simple three-box model, *Dyn. Atmos. Oceans, 21,* 53-82, 1994.

Vaughan, S.L., and K.D. Leaman, The role of small-scale cells in the Mediterranean convection process, *J. Phys. Oceanogr., 25,* 2423-2436, 1995.

Wu, P., and K. Haines, Modelling the dispersal of Levantine Intermediate Water and its role in Mediterranean deep water formation, *J. Geophys. Res., 101,* 6591-6607, 1996.

Wu, P., and K. Haines, The general circulation of the Mediterranean Sea from a 100-year simulation, *J. Geophys. Res., 103,* 1121-1131, 1998.

Wust, G., On the vertical circulation of the Mediterranean Sea, *J. Geophys. Res., 66,* 3261-3271, 1961.

Zavatarelli, M., and G.L. Mellor, A numerical study ofthe Mediterranean Sea circulation, *J. Phys. Oceanogr., 25,* 1384-1414, 1995.

S. Castellari, Istituto Nazionale di Geofisica, Via di Vigna Murata, 605, I-00143 Roma, Italy. (s.castellari@isao.bo.cnr.it)

K. Leaman, Rosenstiel School of Marine and Atmospheric Sciences, University of Miami, 4600 Rickenbacker Cswy., Miami FL 33149. (k.leaman@rsmas.miami.edu)

N. Pinardi, Dipartimento di Fisica, Università degli Studi di Bologna, Viale Berti Pichat 6/2, I-40127 Bologna, Italy. (n.pinardi@isao.bo.cnr.it)

(Received August 25, 1998; revised October 29, 1999; accepted March 6, 2000.)